frontiers in Earth Science

ORIGINAL RESEARCH
published: 03 July 2020
doi: 10.3389/feart.2020.00206

AMS ^{14}C Dating Problem and High-Resolution Geochemical Record in Manzherok Lake Sediment Core From Siberia: Climatic and Environmental Reconstruction for Northwest Altai Over the Past 1,500 Years

Tatiana Blyakharchuk[1], Valerii Udachin[2], Hong-Chun Li[3,4] and Su-Chen Kang[3]*

[1] Institute of Monitoring of Climatic and Ecological Systems, Siberian Branch of Russian Academy of Sciences (IMCES SB RAS), Tomsk, Russia, [2] Institute of Mineralogy, Ural Branch of Russian Academy of Sciences (IM UrB RAS), Tomsk, Russia, [3] Department of Geosciences, National Taiwan University, Taipei, Taiwan, [4] Frontiers Science Center for Deep Ocean Multispheres and Earth System and Key Laboratory of Marine Chemistry Theory and Technology, Ministry of Education, Ocean University of China, Qingdao, China

OPEN ACCESS

Edited by:
Liangcheng Tan,
Chinese Academy of Sciences, China

Reviewed by:
Cheng Peng,
Institute of Earth Environment (CAS), China
Jiawu Zhang,
Lanzhou University, China

***Correspondence:**
Hong-Chun Li
hcli1960@ntu.edu.tw

Specialty section:
This article was submitted to Quaternary Science, Geomorphology and Paleoenvironment, a section of the journal Frontiers in Earth Science

Received: *19 March 2020*
Accepted: *18 May 2020*
Published: *03 July 2020*

Citation:
Blyakharchuk T, Udachin V, Li H-C and Kang S-C (2020) AMS ^{14}C Dating Problem and High-Resolution Geochemical Record in Manzherok Lake Sediment Core From Siberia: Climatic and Environmental Reconstruction for Northwest Altai Over the Past 1,500 Years. Front. Earth Sci. 8:206. doi: 10.3389/feart.2020.00206

This study presents high-resolution multi-proxy biological and geochemical records in an 82-cm sediment core from Manzherok Lake located in a forest–steppe zone on the western piedmonts of Altai Mountain, Russia. Based on ^{210}Pb dating and 48 accelerator mass spectrometry ^{14}C dates as well as pollen data and geochemical proxies, detailed lake history and local climatic changes over 1,500 years are obtained. Prior to the Medieval Warm Period (MWP), the lake had high productivity under stable moderately wet and warm conditions. During 1,150–1,070 year BP, strong surface runoff led to a high detritus input and an increasing lake level, reflecting the onset of MWP. The lake was deep and fresh under the warm and wet conditions of MWP (1,070–850 year BP). In this interval, more aquatic algae and submerged plants on the lake bottom were generated, which would use dissolved CO_2 partially decomposed from organic matters in the deeper sediment layers. Consequently, many acid–base–acid-treated samples contain old carbon influence on their ^{14}C dates. This calls for attention on the chronological construction of lake sediments. During 850–700 year BP, the lake level started to drop with reduced sediment load under cooling and drying conditions. Low sedimentation and lake productivity occurred due to cold and dry climates during 700–500 years BP. Very low sedimentation and hiatus were attributed to ice cover and weak water input between 500 and 50 years BP, corresponding to cold and dry Little Ice Age. Manzherok Lake has recovered productivity and deposition during the current warming century. Change in the total solar irradiance (TSI) is an important factor to influence the climate in the Altai Mountains. With decreased TSI, the Siberian High became strong, which led to the Westerly and the polar front being pushed away from this region, resulting in arid climates. The situation was reversed *vice versa*.

Keywords: radiocarbon dating, pollen, geochemical proxy, lake sediment, Russian altai

INTRODUCTION

A small endorheic or closed lake often leads to a high assimilation potential of living matters, which allows the lake to produce high organogenic masses and to form sapropel-type sediments (Korde, 1960; Popolzin, 1967; Lopatko, 1978). The source materials of sapropel formations in a lake normally include the remains of aquatic organisms such as plankton (phytoplankton and zooplankton), algae, macrophytes, and organic matters as well as mineral substances coming from the catchment area. As organic (humus) substances and inorganic mineral impurities (clay and sand) are introduced into the autochthonous organic matter (formed in the lake) under the influence of biochemical, microbiological, and mechanical processes, sapropel of allochthon origin is formed (Korde, 1960; Vine and Tourtelot, 1970; Lopatko, 1978; Poplavko et al., 1978; Gurari and Gavshin, 1981; Neruchev, 1982; Kuzin, 2007). When interpreting geochemical proxies in lake sediments, it is necessary to identify the source and the migration of those elements and isotopes. For instance, Leonova and Bobrov (2012) studied plankton development in reservoirs of the Siberian region. They revealed that, in small lakes, the organic matter of plankton detritus did not significantly change its micronutrient composition while sinking down to the lake bottom. They quantitatively calculated the supply of chemical elements directly through the "plankton channel" into the lake sediments. Vetrov and Kuznetsova (1997) and Granina (2008) studied the geochemistry of diatom pelagic silts and the microelement composition of plankton in Baikal Lake.

In recent years, interesting work has begun to be devoted to the study of the climatic indicator role of chemical elements in sediments (Syso and Yu, 2007; Kalugin et al., 2014; Darin et al., 2014). Syso and Yu (2007) proposed several geochemical indicators for determining the soil properties. It is believed that the enrichment of lake sapropel by mineral components reflects the enhancement of the surface flow of water (Kalugin et al., 2014). Indicators of this phenomena are considered to be "cluster" elements to which Si, Al, Ti, Fe, Mg, Ca, and K belong. The organic fraction of the sediment is more closely related to the increase of temperature at which the bio-productivity of the catchment basin and the water body increases. Some geochemical indices can be directly used for the paleo-reconstruction of the environment. For example, elements with variable valence can be specific indicators of external conditions (Kalugin et al., 2014). Fe is strictly connected with sulfur in sulfate under anoxic conditions. Additionally, Fe forms siderite in carbonate, whereas Mn-enriched layers mark long-term pauses of sedimentation in oxide systems. The Mo/Mn ratio is correlated well with the anoxic environment. According to Kalugin et al. (2014), the Sr/Rb ratio reflects a portion of clay fraction in annually laminated lake deposits of Shira Lake, which marks a stable sedimentation period in winter time. They divided the elements of the bottom sediments of Lake Shira into three clusters: carbonate (Sr, Sc, and Ca), clastic (Zn, Mo, As, Cu, Ni, U, Nb, Ba, Zr, Ga, Mn, Y, Co, Fe, Ti, Rb, and K), and organic pore water (Br, Cl, and S).

The trace metal elements (TME), heavy metal elements (HME), and rare earth elements (REE) in lake sediments are also used for environmental studies. Li (1991) and Leonova et al. (2010) investigated a number of elements that enrich the upper layers of modern lake deposits relatively to clay shale, including their sources and ways to migration in lake sediments. The groups of elements enriching the upper horizons of lake sapropel with respect to clayey shales are singled out as "highly sapropelophilic" elements (the ash concentration coefficients of which KK = 28–15)—P, Br, Mn, As, and Hg; "sapropelophilic" elements (KK = 7–8)—Fe, Mo, Zn, Cd, Cu, Pb, Ag, and Sb; "weakly sapropelophilic" elements (KK = 2–1)—Se and U; and "non-sapropelophilic" elements (KK <1)—alkaline, alkaline earth elements, and rare earth elements (Leonova et al., 2010). In general, it was found that, in small lakes, the plankton contribution significantly exceeds the supply of the microelements from the plant (macrophytic) source, with the exception of Mn. The share of Mn supply through vegetable detritus is about 15 vs. 1% through the plankton supply channel. Plankton is found as a biogeochemical barrier between the atmosphere and the water surface boundary, which intensively retards the chalcophile elements (Cd, As, Sb, Zn, Pb, Hg, Se, *etc.*) emanating from atmospheric precipitation (Leonova and Bobrov, 2012). Low-biophilic elements of Al, Ti, and Zr are used to characterize the role of clastic and clay material in suspended matter and precipitation (Perelman, 1979).

According to previous studies (Boyarkina et al., 1993; Kutsenogiy and Kutsenogiy, 2000; Raputa et al., 2000; Smolyakov, 2000; Moiseenko et al., 2006), an important additional source of micronutrient supply in small closed lakes is atmospheric mineral matter, and the role of the plankton biofilter is very strongly manifested in such environments (Leonova and Bobrov, 2012). Phyto- and zooplankton are mainly the first substance (biofilter) which involves chemical elements in the biological cycle at the atmosphere–water interface. On this barrier, phyto- and zooplankton get enriched by chalcophile elements which enter the water surface of lakes mainly as part of atmospheric precipitation. These elements are separated into a group of so-called "volatile" elements (Malakhov and Makhonko, 1990; Shotyk et al., 1996; Gavshin et al., 2004; Bobrov, 2007; Dauvalter et al., 2008; Bobrov et al., 2011). While precipitating on the earth's surface as part of atmospheric aerosols, chalcophile "volatile" elements get actively induced in the processes of biodifferentiation by living matter as well as by plankton in small lakes (Leonova et al., 2006; Bobrov et al., 2007). The further fate of these elements is determined by the hydrochemical characteristics of the lake water. Moreover, these elements enter the bottom sediments of the plankton detrital composition if the hydrocarbonate class of water shows a pH range of 7–8 (Leonova et al., 2008, 2011; Leonova and Bobrov, 2012). In lakes with sulfate class of water with low pH ranging 5–6, these elements would be leached out from plankton detritus into an aqueous solution and get re-introduced into trophic chains. As, Se, Cd, Hg, and Pb are toxic elements with extremely low background concentrations in water. However, they are characterized by high accumulation coefficients in living organisms (Leonova and Bychinsky, 1998; Leonova, 2004; Leonova et al., 2007). Sc, Zr, Nb, Hf, and Th are included in the group of terrigenous elements. Sc is characterized by low solubility, and it has been suggested

to use, for standardization, the basic elements to evaluate the accumulation of elements in various water bodies using the "enrichment factor" (Shotyk et al., 1996).

In Blyakharchuk et al. (2017), detailed palaeopollen and diatom data and brief elemental data with 21 accelerator mass spectrometry (AMS) ^{14}C dates in an 82-cm sediment core from Manzherok Lake located in a forest–steppe zone on the western piedmonts of Altai Mountain were used for climate and environmental reconstruction over the last 1,400 years. Among the 21 ^{14}C dates, nine non-acid–base–acid (ABA)-treated samples are older than their ABA-treated pairs, even though the ABA-treated samples show a rather scattered chronological stratigraphy (Blyakharchuk et al., 2017). Thus, we have dated more layers with ABA treatment. In this study, a total of 48 AMS ^{14}C dates plus ^{210}Pb dating results from the 82-cm core yield better chronology. The present study reveals detailed TME, HME, and REE contents in the core. Together with physical, biological, and geochemical data sets, a detailed history of the lake and the environmental conditions under climate influence over the past 1,500 years has been discussed. In addition, archeological activity and human impact in the study area will be addressed.

AREA OF STUDY

Manzherok Lake [51.822° N, 85.811° E, 373 m above sea level (a.s.l.)] is a small, freshwater lake located in the western periphery of the Altai Mountains of Southern Siberia on a terrace of the right-hand bend of the Katun' River, 18 km southwest of Gorno-Altaisk City (51°49′15.5" N, 85°48′35.7" E, 423 m a.s.l.) (**Figure 1**). The lake has an elevation of 373 m, which is much higher than that of Katun' River (297 m a.s.l.). Therefore, although the lake is about 2 km away from the river, there is no evidence that the river has invaded the lake over the late Holocene. Geologically, Manzherok Lake lies within the tectonic unit of Bijsk-Katun' anticlinorium—exhibiting more ancient geological structures of the Altai Early Caledonian fold system. Consequently, in the area of Manzherok Lake, a positive element of relief is presented by ancient carbonate rocks of the Baratalsk series (R3-V), formed in the Proterozoik marine environment (Geology of the USSA, 1997). The low mountains around the lake are covered by forest–steppe vegetation with *Betula pendula* (BP) and *Pinus sylvestris*, with patches of *Pinus sibirica*. The climate is moist with a relatively mild temperature even though it is classified as of the West Siberian continental type (Ogureeva, 1980). A more detailed regional setting with detailed pollen and diatom data of Manzherok Lake is presented in an earlier publication (Blyakharchuk et al., 2017).

Although the origin and the history of Manzherok is still under study, Rusanov and Vazhov (2017) provided the most comprehensive summary of the Manzherok Lake studies. The origin of Lake Manzherok was probably caused by a catastrophic breakthrough of the large glacial-dammed lakes of Altai at the

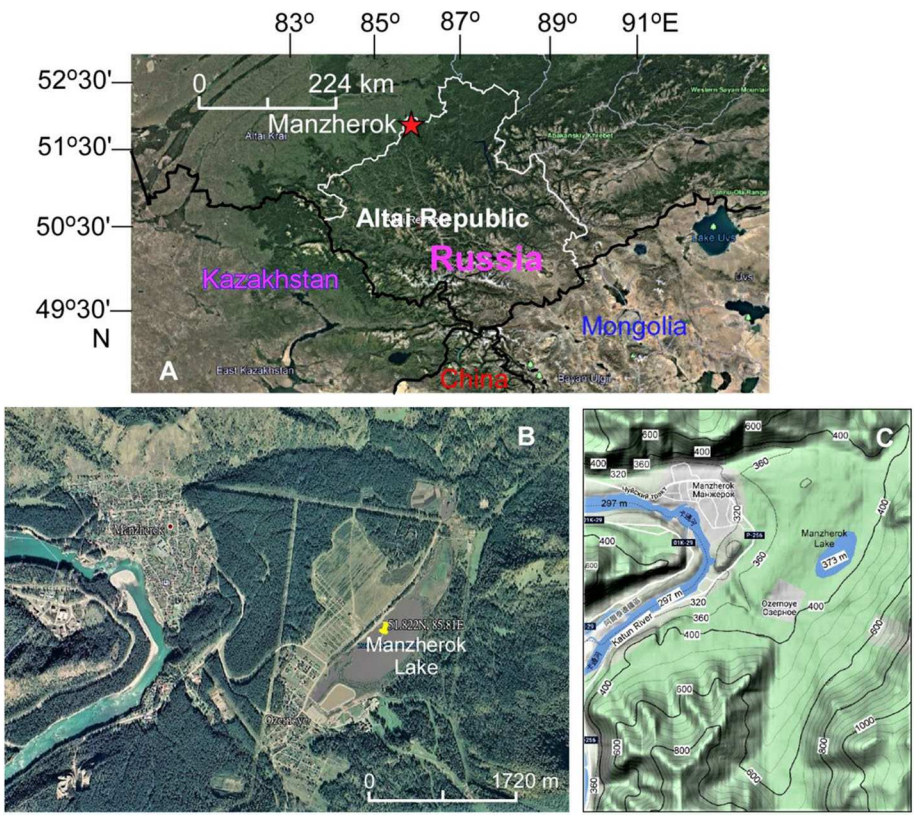

FIGURE 1 | Location of the study area. **(A)** Map of Altai and the surrounding areas. **(B)** Satellite map of the Manzherok area. **(C)** Topographic map with contour lines of the Manzherok area. The figures are modified from maps that have been downloaded from Google Map.

end of the Ice Age. Fed by streams flowing from the surrounding slopes, precipitation, and groundwater, the lake is elliptical in shape and elongated from southwest to northeast. Manzherok Lake is a freshwater open lake, with an outlet at the southwest end through a swampy runoff hollow. The lake water has low pH of 6.2–7.2 and contains low ionic concentrations. The salinity and the alkalinity of the lake are quite low, e.g., CO_3^{2-} and HCO_3^- measurements in the lake in 1972 were 0.0 (non-detectable) and 0.28 mg/100 g water, respectively (Ilyin, 1982). The modern Manzherok Lake is a popular recreation area. Human activities around the lake, such as fishing, farming, and grazing, may have impact on the sedimentary processes to the lake.

METHODS

Elemental Geochemical Analyses of Lake Sediment Samples

About 0.05 g of dry powder lake sediment from every 1-cm horizon of the upper 31-cm section and every 2-cm interval of the 32–82-cm section of the core was precisely weighted and then digested with a mixed acid solution ($HF + HNO_3 + HCl$) in a polytetrafluoroethylene beaker using a microwave system (SpeedWave 3, Berghof, Germany). The microwave program ran for 15 min at about 145°C, for 20 min at 200°C, and a holding time of 15 min, followed by a cool-down procedure of 10 min. After the residue was completely diluted, the evaporate was dissolved repeatedly with concentrated HCl to convert the solution in chloride medium. Then, the solution was diluted to 100 ml volume with 0.5 N HCl. The acid solution was filtered through an acetate filter membrane with 0.45-μm pore size to remove any undissolved particles. The filtered solution was analyzed for 45 elements using inductively coupled plasma-mass spectrometry (Agilent Technologies 7700×, Japan).

Multi-element standards (Agilent) were routinely analyzed as quality control. The analytical performance was assessed through related materials including lake Baikal sediment reference material BIL-1 (Russia) and LKSD-1 (Canada), which all have certified or recommended values. The relative standard deviation was <8%. The recovery of the reference materials ranges 91–112%. A total of 54 samples have been analyzed for TME, HME, and REE.

^{210}Pb Dating and Sedimentation Models

Lead-210 measurement can be achieved by either directly using low-background gamma spectrometry or measuring its decay product (^{210}Po) via alpha spectrometry. Despite being proven efficient for low-density samples (e.g., peat, lake sediment), gamma spectrometry is limited in small samples (e.g., Ebaid and Khater, 2006), while the measurement of low-energy ^{210}Pb gamma photons ($E_{210Pb} = 46.5$ keV) is virtually impossible. The ^{210}Pb dating of the Manzherok Lake core was determined by the ^{210}Po method (Pawlyta et al., 2004; Cooke et al., 2007; Baskaran et al., 2014).

Dry sediment samples of 1.0 g for the top core section and 2.0 g for the bottom position with a known amount of ^{209}Po spike solution were placed into Teflon vessels and digested at a temperature of 120°C using concentrated $HNO_3 + HClO_4 +$ HF. After 12 h of digestion, the solution was centrifuged. The supernatant was transferred into a Teflon beaker and evaporated with 6 M HCl until dryness. The evaporate in the Teflon beaker was dissolved in 10 ml 0.5 N HCl and transferred into a 50-ml centrifuge tube. Ascorbic acid powder was added into the solution to form Fe complex ions in order to prevent the Fe ions to be co-precipitated with Po ions. A silver disk, 8 mm in diameter, was placed in the solution of the centrifuge tube. Then, the centrifuge tube was placed in a water bath at 60°C. Polonium isotopes were spontaneously deposited within 4 h on the Ag disk. The activities of ^{209}Po and ^{210}Po were measured by an alpha spectrometer. Two blank samples were analyzed with each sample batch to verify the quality of the chemical extraction. The procedure of acid extraction and deposition of polonium was outlined in Suriyanarayanan et al. (2008) and Ugur et al. (2003). The total ^{210}Pb activity reached a relatively constant below 13 cm in depth (**Figure 2**). We use the average ^{210}Pb activity below the 13-cm depth as the supported ^{210}Pb activity. The excessive ^{210}Pb ($^{210}Pb_{ex}$) in each sample was obtained by the measured total activity of ^{210}Pb subtracted by the supported ^{210}Pb activity (**Figure 2**). The Constant Rate of Supply model (Appleby, 2001) was applied to the ^{210}Pb inventories calculated from the $^{210}Pb_{ex}$ data to generate ages.

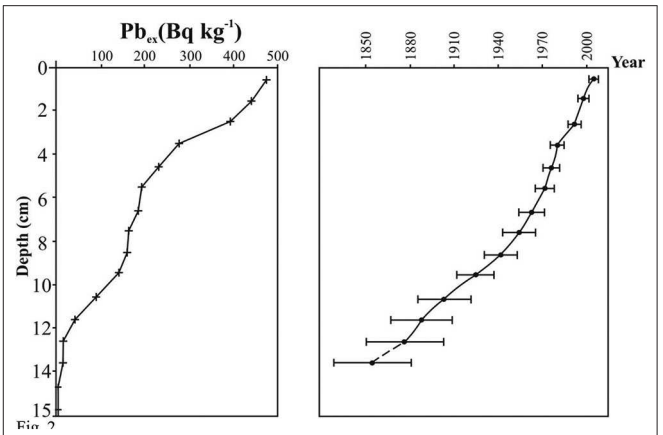

FIGURE 2 | Vertical profiles of ^{210}Pbex of Manzherok Lake sediment core and ^{210}Pb chronologies. The dashed line indicates an interpolation result of age (see text for interpretation).

AMS Radiocarbon Dating

In Blyakharchuk et al. (2017), we reported 21 AMS ^{14}C dates from the core. In that study, we have found that the lake sediments need ABA treatment (Brock et al., 2010). Otherwise, the ^{14}C dates became older than their true ages. Therefore, in the present study, about 0.1 g of bulk gyttja sample from different depths of the core was treated with 0.5 N HCl, 0.5 M NaOH, and 0.5 N HCl sequentially. The dry-treated sample was then placed into a 9-mm quartz tube with pre-combusted CuO powder and a piece of silver and then placed on a vacuum line. The quartz tube was sealed under vacuum of 1e-5 mbar and then combusted for 6 h at 850°C in a muffle furnace. The CO_2 produced by oxidation was transferred and purified cryogenically on the vacuum line

and sealed into combination tubes, which included a 9-mm glass tube with Zn and TiH_2 powders and an inner 6-mm center tube containing Fe powder (Xu et al., 2007). Graphitization of the CO_2 in the tube took place in the muffle furnace at 550°C for 6 h.

Sample graphite was pressed into a target holder and measured for its $^{14}C/^{12}C$ and $^{13}C/^{12}C$ ratios with a 1.0 MV Tandetron Model 4110 BO-Accelerator Mass Spectrometer in the NTUAMS Lab. Every sample batch contains at least three international standards (OXII, 4,900 C), three backgrounds (BKG), and two inter-comparison samples (IRIs). The measurement mode was $^{14}C^{3+}$ to avoid $2Li^{+}$ interference with $^{14}C^{2+}$. Using the $^{14}C/^{12}C$ and the $^{13}C/^{12}C$ ratios of OXII, BKG, and the samples, the percentages of modern carbon (pMC), $D^{14}C$ (= pMC/100–1) × 1,000, and ^{14}C conventional age were calculated with the Libby half-life of 5,568 years (Stuiver and Polach, 1977). $\delta(^{13}C)$ is calculated from the $^{13}C/^{12}C$ ratios of OXII ($\delta^{13}C = -18‰$) and sample, which is used for the correction of carbon isotopic fractionation (against −25‰) during natural and AMS dating laboratory processes. Hence, the $\delta(^{13}C)$ value is not only determined by the carbon isotopic composition of the sample but also strongly influenced by the ABA treatment and the AMS measurement. Measured by AMS, the $\delta(^{13}C)$ is different from $\delta^{13}C$ (measured by isotope-ratio mass spectrometry) and cannot be used for stable isotope interpretation. The conventional age is transferred into calibrated ^{14}C ages with 1σ error using the calibration curve IntCal13 (Stuiver and Reimer, 1993; Niu et al., 2013; Reimer et al., 2013). The ^{14}C ages expressed in this paper are calibrated ^{14}C ages in years BP (0 year BP = 1,950 CE). A total of 48 AMS ^{14}C dates from the core are listed in **Table 1**.

RESULTS AND DISCUSSIONS

Problems of ^{14}C Dates and New Chronology

Table 1 and **Figure 3** show all the ^{14}C dates. First of all, the core contains very high organic content (>20 wt.%) (**Figure 3B**). The core materials have black color with swamp odor, which look totally different from the river sediments and the surrounding debris. The latter ones contain much lower organic matter. The materials in the core are very suitable for ^{14}C dating, especially the lower part which contains organic matter like peat as high as 35 wt.%. However, these organic matters are well-decomposed and difficult to be isolated from the bulk sediments. In the earlier publication (Blyakharchuk et al., 2017), several plant remain samples were AMS ^{14}C dated, even though those plant remains still show old carbon influence on the non-ABA treated ^{14}C dates (**Table 1**). In fact, all non-ABA-treated samples have older ages than those of ABA-treated samples from the same bulk sample pairs. Since the remaining core materials could not pick up more plant remains, in this study we have dated bulk gyttja (sapropel) samples from multiple horizons above 35 cm in depth, with ABA pre-treatment. As the lake sediments were deposited stratigraphically, their ages should become older from top to bottom. In **Table 1**, the first criterion for selecting the corrected dates is to remove all the non-ABA treated samples. The second criterion is to remove an older date (ABA-treated) in the upper layer as the younger dates contain least old carbon influence. If an age in the upper layer is slightly older that in the level below but is within uncertainties, we will keep it.

Although the lake has low pH (6.2–7.2), the carbonate content in the bulk sample still has about 2–5% (**Figure 3**). Those carbonates contain normally old carbon from detritus carried by surface runoff. With ABA treatment, those carbonates can be removed. Another older carbon source comes from organic carbon such as humic acids and/or CO_2 decomposed from deeper sediments. The humic acids decomposed from older organic matter in the deeper sediments may migrate upward and enter the bulk gyttja. The function of base treatment in the ABA procedure is to remove such mobile humic acids. Thus, the ABA-treated samples should be able to eliminate the influence of carbonate and mobile humic acid. However, there are many newly measured ABA-treated samples showing reversed ^{14}C ages (**Table 1** and **Figure 3**). Our hypothesis of this old carbon influence is that dissolved CO_2 in the lake water contained CO_2 decomposed from organic matters in the deeper sediments that was uptaken by submerged plants and aquatic algae to form organic compounds which could not be removed by ABA treatment.

Since the CO_2 decomposed from organic matters in the deeper sediments is a function of lake chemistry such as redox condition, water temperature, pH, and bacterial activity, *etc*., the later ones are affected by water depth and climatic condition. Thus, this old carbon influence is different from "hard water effect" or "reservoir effect." "Hard water effect" is caused by high concentrations of HCO_3^- and CO_3^{2-} in lake water, which commonly exist in closed alkaline lakes. Manzherok Lake does not belong to such a lake. "Reservoir effect" including hard water effect sometimes can be caused by organic carbon input from inflow sediments, for example, Teletskoye Lake in Altai has reservoir age in the ^{14}C ages of bulk organic carbon in the sediments (Rudaya et al., 2016). This lake is also a freshwater lake, but its sediments contain a low percentage of total organic carbon. A total of 16 AMS ^{14}C dates (from two labs) on the TOC of bulk sediments from the lake core show about 2,400–3,000 years of "reservoir age" throughout the sediment core. This is not the case for Manzherok Lake core. In the Manzherok Lake core, there are several ^{14}C dates from plant remains. Even on the bulk gyttja samples from the upper 5-cm part, four ABA-treated samples contain nuclear bomb ^{14}C signal, indicating no reservoir effect (**Table 1**). Thus, the old carbon influence on the ^{14}C age of the Manzherok Lake sediments is not considered as "hard water effect" or "reservoir effect." This influence varies with lake condition with time. **Figure 3A** shows that the old carbon influence was negligible above 19 cm in depth and was relatively weak below 46 cm in depth.

In general, deeper water (higher lake level) is in favor of the anoxic condition in the bottom of the lake. Warmer lake water provides a stronger bacterial activity. The reduced environment would generate CH_4, which would be oxidized into CO_2 during degassing in the lake bottom. In **Figure 3**, most ABA-treated samples with rejected ^{14}C ages are in 40–20-cm depths. This interval belongs to the Medieval Warm Period (MWP). In later

TABLE 1 | Accelerator mass spectrometry ^{14}C dates of the samples from Manzherok Lake core.

Lab code	Sample ID	Depth (cm)	Pretreatment	pMC (%)	^{14}C age (year BP)	Calibrated ^{14}C age (year BP)	$\delta(^{13}C)$ ‰	Type
NTUAMS-3319	MZh 1-2 Pb	1.5	ABA	100.09 ± 1.15	−8 ± 92	Modern	−19.88	Bulk gyttja
NTUAMS-3320	MZh 2-3	2.5	ABA	101.88 ± 0.79	−150 ± 62	Modern	−18.24	Bulk gyttja
NTUAMS-3321	MZh 3-4	3.5	ABA	100.48 ± 0.79	−38 ± 63	Modern	−21.51	Bulk gyttja
NTUAMS-2876	MZh 4-5	4.5	No ABA	98.17 ± 0.72	149 ± 58	145 ± 60*	−25.39	Peat
NTUAMS-2876c	MZh 4-5	4.5	ABA	101.73 ± 0.81	−138 ± 64	Modern	−24.06	Peat
NTUAMS-3322	MZh 5-6	5.5	ABA	94.92 ± 0.75	419 ± 63	505 ± 60	−15.41	Bulk gyttja
NTUAMS-3323	MZh 6-7	6.5	ABA	95.90 ± 0.81	337 ± 68	390 ± 115	−34.75	Bulk gyttja
NTUAMS-3324	MZh 8-9 Pb	8.5	ABA	93.39 ± 1.15	550 ± 99	580 ± 130	−18.59	Bulk gyttja
NTUAMS-3325	MZh 9-10	9.5	ABA	90.43 ± 0.76	808 ± 67	720 ± 30	−31.19	Bulk gyttja
NTUAMS-3326	MZh 11-12	11.5	ABA	90.78 ± 0.72	777 ± 64	710 ± 80	−24.60	Bulk gyttja
NTUAMS-3327	MZh 12-13	12.5	ABA	91.72 ± 0.73	694 ± 64	670 ± 90	−17.95	Bulk gyttja
NTUAMS-3328	MZh 13-14	13.5	ABA	90.28 ± 0.74	821 ± 65	730 ± 30	−36.07	Bulk gyttja
NTUAMS-3329	MZh 14-15	14.5	ABA	91.82 ± 0.73	686 ± 63	670 ± 85	−29.53	Bulk gyttja
NTUAMS-3330	MZh 16-17 Pb	16.5	ABA	88.84 ± 0.77	950 ± 69	875 ± 125	−43.56	Bulk gyttja
NTUAMS-3331	MZh 17-18	17.5	ABA	89.06 ± 0.71	931 ± 64	860 ± 115	−25.09	Bulk gyttja
NTUAMS-3332	MZh 18-19	18.5	ABA	89.02 ± 0.75	935 ± 65	860 ± 115	−34.75	Bulk gyttja
NTUAMS-3333	MZh 19-20	19.5	ABA	85.79 ± 0.66	1,231 ± 61	1,175 ± 120#	−14.62	Bulk gyttja
NTUAMS-3335	MZh 21-22	21.5	ABA	85.81 ± 0.71	1,229 ± 66	1,175 ± 120#	−35.51	Bulk gyttja
NTUAMS-3336	MZh 22-23	22.5	ABA	86.71 ± 0.67	1,146 ± 62	1,040 ± 125#	−24.81	Bulk gyttja
NTUAMS-3337	MZh 23-24	23.5	ABA	85.93 ± 0.68	1,218 ± 64	1,140 ± 120#	−32.04	Bulk gyttja
NTUAMS-2877	MZh 25-26,	25.5	Partial ABA	84.81 ± 0.66	1,323 ± 63	1,280 ± 85*	−37.75	Bulk gyttja
NTUAMS-2877b	MZh 25-26	25.5	ABA	89.09 ± 0.72	928 ± 65	855 ± 115	−19.41	Bulk gyttja
NTUAMS-3248	MZh 26-27	26.5	ABA	86.74 ± 0.70	1,142 ± 65	1,040 ± 130#	−33.74	Bulk gyttja
NTUAMS-3249	MZh 27-28	27.5	ABA	85.44 ± 0.77	1,264 ± 73	1,225 ± 130#	−35.34	Bulk gyttja
NTUAMS-2920	MZh 28-29,	28.5	No ABA	84.70 ± 0.54	1,334 ± 51	1,290 ± 85*	−25.30	Bulk gyttja
NTUAMS-2920b	MZh 28-29	28.5	ABA	87.73 ± 0.70	1,051 ± 64	980 ± 145	−15.67	Bulk gyttja
NTUAMS-3250	MZh 28-29	28.5	ABA	89.02 ± 0.70	934 ± 63	860 ± 115	−36.75	Bulk gyttja
NTUAMS-3251	MZh 29-30	29.5	ABA	85.85 ± 0.67	1,226 ± 63	1,165 ± 130	−28.52	Bulk gyttja
NTUAMS-3253	MZh 30-31	30.5	ABA	83.14 ± 0.92	1,483 ± 88	1,370 ± 150#	−12.37	Bulk gyttja
NTUAMS-3254	MZh 31-32	31.5	ABA	85.19 ± 0.93	1,288 ± 88	1,235 ± 150#	−15.54	Bulk gyttja
NTUAMS-3255	MZh 32-33	32.5	ABA	85.28 ± 0.92	1,280 ± 87	1,230 ± 145#	−17.04	Bulk gyttja
NTUAMS-3255	MZh 33-34	33.5	ABA	85.59 ± 0.92	1,250 ± 86	1,215 ± 130#	−14.97	Bulk gyttja
NTUAMS-3256	MZh 34-35	34.5	ABA	83.41 ± 0.91	1,457 ± 88	1,350 ± 145#	−18.32	Bulk gyttja
NTUAMS-2878	MZh 39-40	39.5	ABA	96.12 ± 0.61	318 ± 51	380 ± 95*	−25.71	Plant remain
IAAA-150551		40.5	No ABA		1,550 ± 20	1,460 ± 35*	−27.94	Bulk gyttja
NTUAMS-2917	MZh Sc 46-47	46.5	No ABA	84.63 ± 0.59	1,341 ± 56	1,290 ± 90*	−16.72	Macrofossils
NTUAMS-2917b	MZh 46-47	46.5	ABA	86.74 ± 0.74	1,143 ± 68	1,065 ± 130	−32.68	Macrofossils
NTUAMS-2879	MZh Sc-53-54	53.5	ABA	83.67 ± 0.57	1,432 ± 55	1,330 ± 35#	−39.42	Macrofossils
NTUAMS-2880	MZh 60-61	60.5	ABA	85.27 ± 0.55	1,280 ± 52	1,230 ± 70	−33.10	Plant remain
NTUAMS-2918	MZh Sc-63-64,	63.5	No ABA	80.53 ± 0.57	1,740 ± 57	1,660 ± 105*	−24.44	Macrofossils
NTUAMS-2918b	MZh Sc 63-64	63.5	ABA	82.23 ± 0.66	1,572 ± 64	1,470 ± 120#	−17.51	Macrofossils
NTUAMS-2921	MZh 70-71	70.5	No ABA	80.88 ± 0.51	1,705 ± 50	1,605 ± 105*	−21.25	Bulk gyttja
NTUAMS-2921b	MZh 70-71	70.5	ABA	85.29 ± 0.84	1,278 ± 80	1,215 ± 140	−37.39	Bulk gyttja
NSK_UGAMS-21783		70.5	No ABA		1,742 ± 22	1,660 ± 55*	−32.10	Bulk gyttja
NTUAMS-2881	MZh 71-72	71.5	ABA	84.44 ± 0.64	1,358 ± 61	1,295 ± 90	−45.75	Plant remain
NTUAMS-2919	MZh Sc-72-73	72.5	No ABA	79.80 ± 0.51	1,813 ± 51	1,765 ± 100*	−37.06	Bulk gyttja
NTUAMS-2919b	MZh Sc 72-73	72.5	ABA	82.54 ± 0.66	1,541 ± 64	1,445 ± 120	−20.44	Bulk gyttja
IAAA-150552		81.5		83.38 ± 1.14	1,460 ± 20	1,350 ± 35	−17.51	Plant remain

*The symbols * and # mean that the dates are rejected in the chronological construction due to possible multiple carbon sources.*
The errors for percent of modern carbon (pMC) and measured ^{14}C age are 2σ error. The calibrated ^{14}C ages with 1σ error are used in the IntCal13 curve. ABA stands for acid–base–acid treatment.

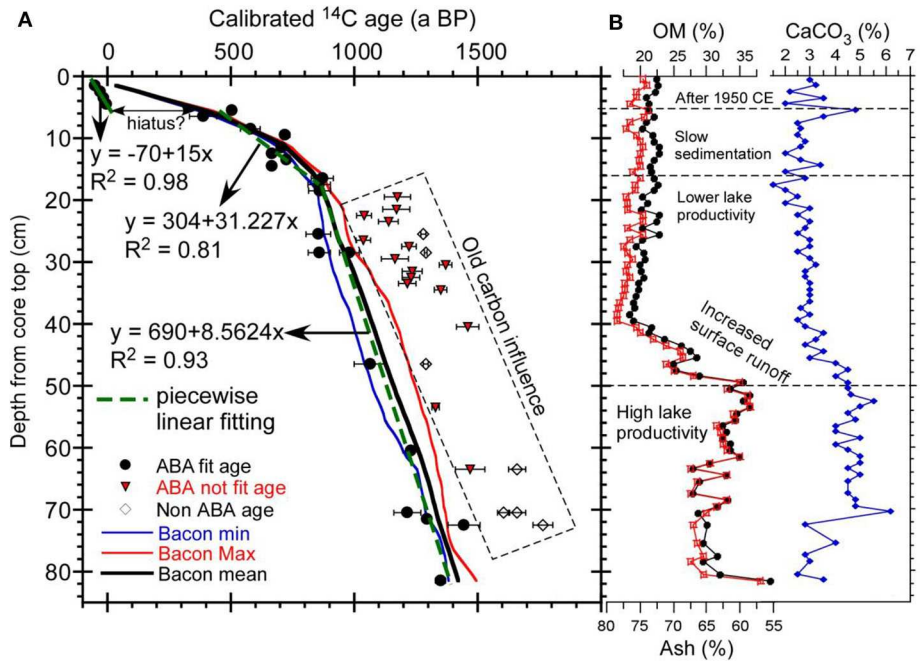

FIGURE 3 | (A) Accelerator mass spectrometry ^{14}C dating and chronology of the core. The three linear equations are used in available ^{14}C ages in three segments: 0–5, 6–20, and 20–82 cm. **(B)** Organic matter (OM, black), ash (red), and $CaCO_3$ contents of the core. Note that the scale axis of OM and ash are opposite so that one can see the lake sediments that contain mainly OM and detritus, which are linearly negatively correlated ($R^2 = 0.99$).

sections, we will interpret that this interval had a higher lake level under warm and wet climatic conditions. Since the lake sediments should be deposited in age sequence, those reversed ages could not be used for chronology construction. Based on the criteria described above, we remain as many reasonable ^{14}C dates as possible for the Bacon age model (Blaauw and Christen, 2011). **Figure 4** exhibits the Bacon age model of the Manzherok Lake core, which shows the core to contain deposition from 1,440 years BP to the present.

Our findings about the problems of ^{14}C dating on the Manzherok Lake sediments call for attention about chronological construction: (1) it is necessary to perform ABA treatment for lake sediments and (2) ABA treatment cannot remove old carbon influence if uptake is older dissolved CO_2 (non-equilibrium with the atmospheric CO_2) by organisms in the lake. In freshwater lakes, terrestrial plant remains in lake cores are often difficult to be obtained for dating. Old carbon influence and age reversion are common, e.g., in Rudaya et al. (2016). Sometimes, with a few ^{14}C dates, the chronology may be not good even if the dates are in a stratigraphic order.

Although the new Bacon age model provides a better chronology than that in Blyakharchuk et al. (2017), it has a problem in the upper 5-cm part. The Bacon age model results yielded ages in the upper 5-cm part of 0–305 years BP. However, four ^{14}C dates in the upper 5 cm show nuclear bomb ^{14}C, reflecting that the lake sediments in this interval must be deposited after 1,950 CE. The ^{14}C ages from 5- to 9-cm depths quickly jumped to 390–580 years BP, indicating that the lake deposition between 5- and 7-cm depths could have hiatus. Because the Bacon age model does not allow sedimentary hiatus, the modeled result forces the ages in the upper 5 cm to become older. Besides that, the ^{210}Pb dating result also indicates that the upper 10-cm part has an apparent $^{210}Pb_{ex}$ decay trend, reflecting modern deposition (**Figure 2**). Therefore, the results of the Bacon age model for the upper 5-cm part were not used. We instead use a linear sedimentation rate given by the ^{210}Pb dating for the upper 5-cm part. The reason that we do not use the ^{210}Pb ages shown in **Figure 2** is that ^{210}Pb in the surface sediments of a freshwater lake can diffuse downward (Benoit and Hemond, 1991), whereas the majority of the organic carbon (plant remains) in the lake sediments are not mobile. Hence, we use the age–depth relationship of the Bacon age model below the 5-cm depth. In the new chronology, there is only one data point (1-cm layer) between 0 year BP (4.5-cm depth) and 465 years BP (6.5-cm depth). This interval represents the depositional period of the Little Ice Age. Nevertheless, the new chronology is significantly improved by more ^{14}C dates and ^{210}Pb. We shall re-interpret the Manzherok Lake record based on the new chronology.

Spore–Pollen Data for Manzherok Lake

A detailed spore–pollen diagram, with descriptions of the pollen zones and the phases of vegetation development in the study area obtained from the Lake Manzherok core, was published earlier (Blyakharchuk et al., 2017). According to the new chronology, the time boundaries of the phases in vegetation development reconstructed based on the pollen zones have changed slightly (**Figure 5**), which can be summarized as follows:

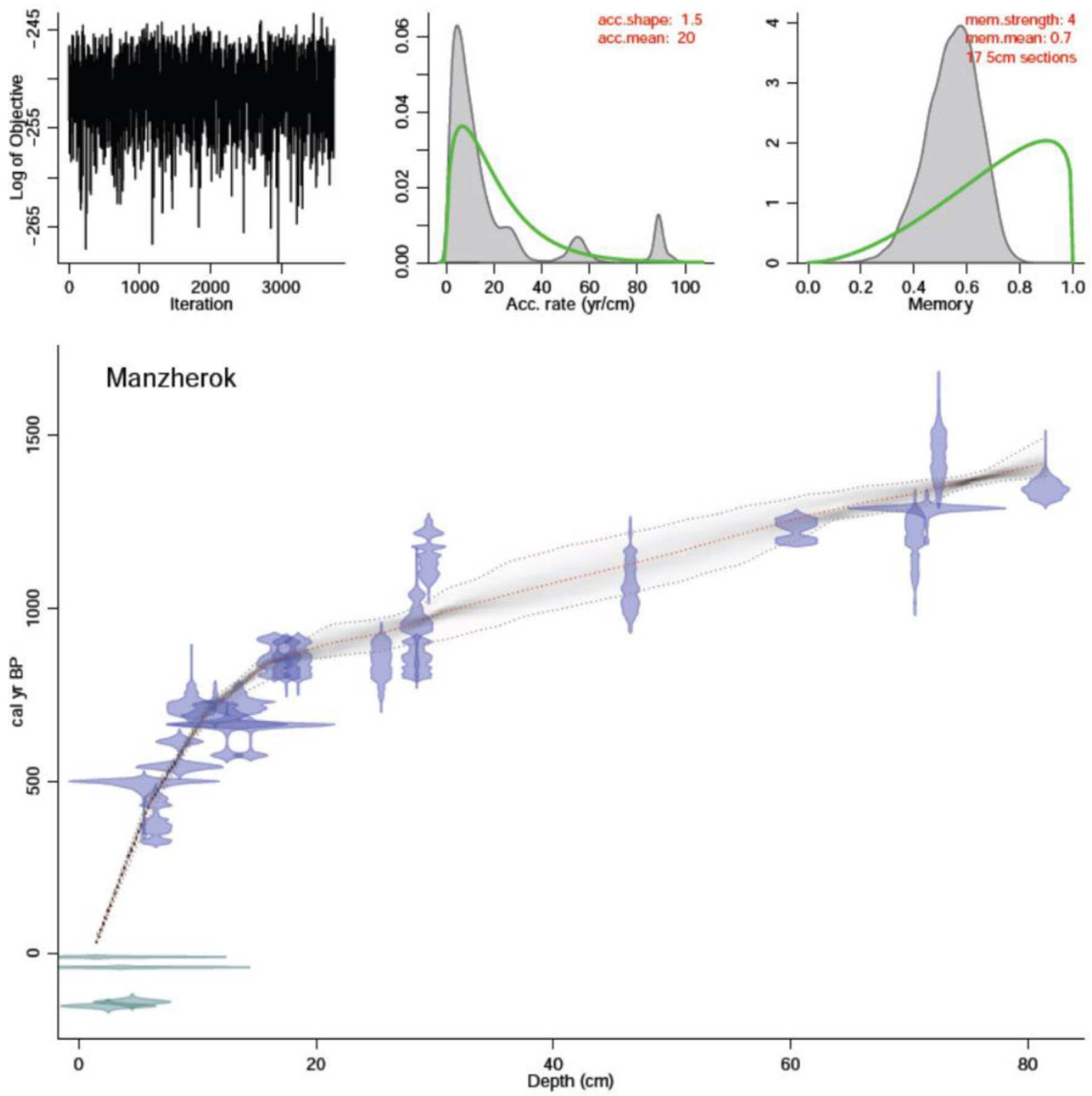

FIGURE 4 | Bacon model result (see text for evaluation of the result).

1. The phase of the birch forest–steppe (pollen zone 1 at 82–50 cm) now is dated 1,440–1,150 years BP or VI–IX centuries AD. (In old chronology, it was 1,350–1,200 years BP).
2. The transitional phase from the birch forest–steppe to birch and pine forests (pollen zone 2 at 50–40 cm) took place at 1,150–1,070 years BP or IX–X centuries AD. (In old chronology, it was 12,00–1,150 years BP).
3. The phase of the birch and pine forests (pollen zone 3 at 40–20 cm) now is dated 1,070–850 years BP or X–XII centuries AD. (In old chronology, it was 1,100–700 years BP).
4. The phase of the pine–birch forest–steppe (pollen zone 4 at 20-cm depth to the surface) now is 850 a BP—contemporary. (In old chronology, it was 700 a BP—contemporary).

Based on the Manzherok pollen data, we reconstruct climate changes in terms of humidity and compare with neighboring palaeoecological data of Teletskoye Lake record (Rudaya et al., 2016) (**Figure 6**). Although the new chronology practically has no significant influence on the interpretations which were made in Blyakharchuk et al. (2017), some differences are addressed below:

1. According to the modified chronology, the period of humid climates during medieval episode became shorter than that in the previous chronology (200 years compared with 400 years). Consequently, it can be concluded that the climate of the medieval climatic anomaly in the western foothills of the Altai was not uniform in terms of the degree of wetness. The early Middle Ages (1,050–900 years BP) was wet, which is marked by the spread of dark coniferous

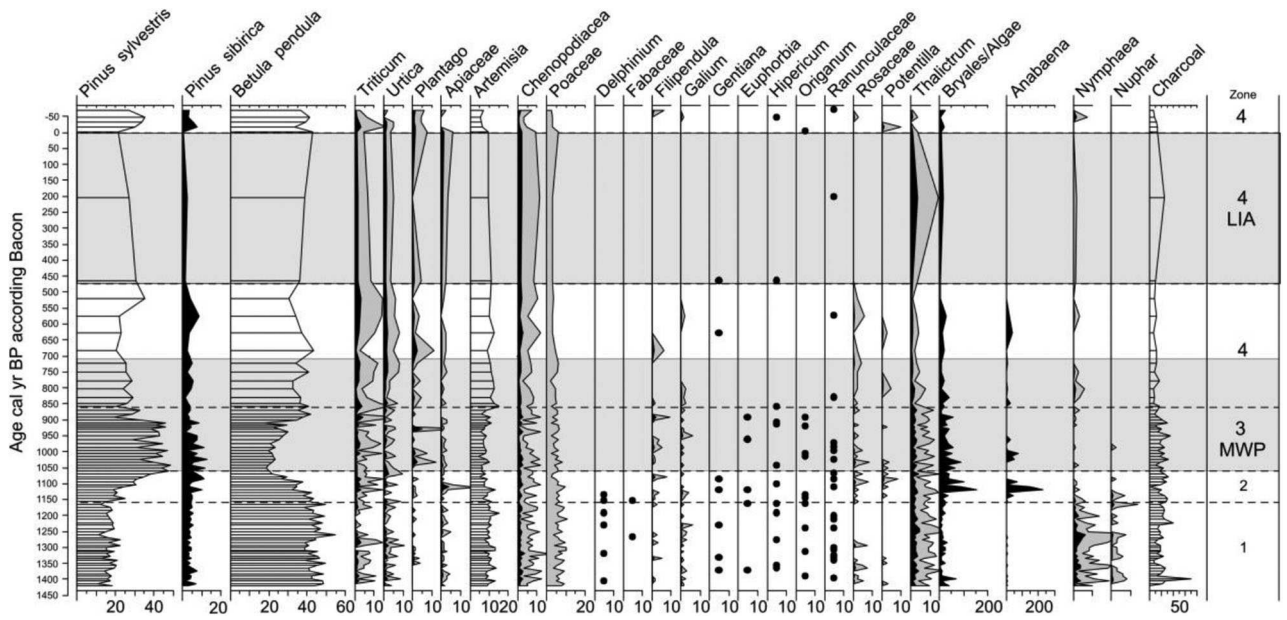

FIGURE 5 | Pollen diagram of Manzherok Lake on even time scale. The pollen types are presented in % from the pollen of terrestrial plants.

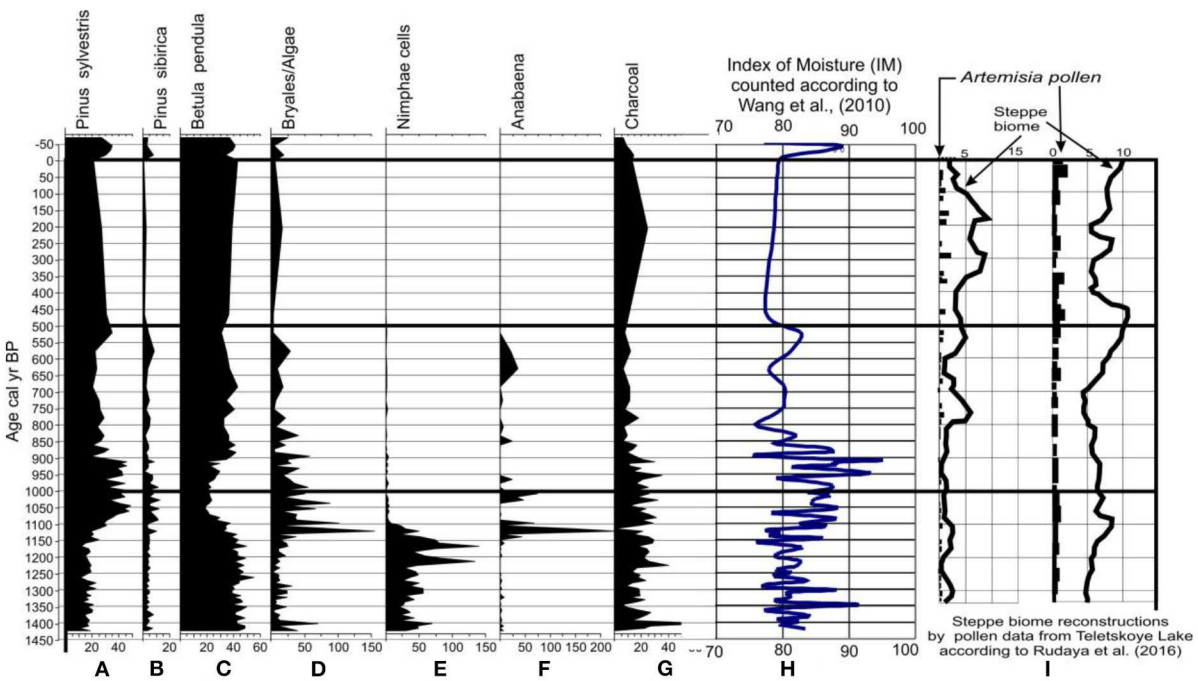

FIGURE 6 | Diagnostic palynomophs of Manzherok Lake and the pollen-based index of humidity of the climate from this study compared with the content of diagnostic *Artemisia* pollen and steppe biome reconstructions in the neighboring Teletskoye Lake (Rudaya et al., 2016). (**A-I**) indicator pollen types and indices based on pollen.

and pine forests in the vicinity of the Manzherok Lake. The late Middle Ages (900–700 years BP) was characterized by relatively dry climate and domination of the birch forest–steppe.

2. The Mongolian invasion (1,236–1,242 years CE) in the territory of Altai to the new chronology is synchronous with the layer of lake sediment at the depth of 11–13 cm or ∼710 years BP (25–30 cm in the old version). During this period,

the climate became less arid than before, and the area occupied by wormwood steppes in the foothills of the Altai decreased. Below this layer of sediment (850–750 years BP), a new series of geochemical data shows two high maxima of Zn and an increase of Cu and Fe content. In the pollen spectrum of this layer, the abundance of pollen of anthropogenic indicators and charcoal was slightly decreased. These indicators confirm our earlier interpretation of the influence of Mongolian invasion on the Altai region (Blyakharchuk et al., 2017).

3. During the cold Little Ice Age (LIA), according to the modified chronology, the rate of sediment accumulation in Manzherok Lake was very low or even absent. The cold and dry climates during LIA could lead to a longer period of frozen lake surface and very low biological productivity in the lake. Low surface runoff under the dry climates reduced the sediment input into the lake. Unfortunately, based on the new chronology, there is only a 2-cm layer falling into LIA. Thus, it is not possible to trace the detailed effect of LIA climates on the lake deposition by biological and geochemical proxies. Besides the very low sedimentation which indicates cold/dry climatic condition, our interpretation on the biological and geochemical results of the 5–7-cm sediment sample deposited during the LIA should be with caution.

Results of High-Resolution Geochemical Analysis

In this study, a new and detailed series of geochemical data (**Table 2**) was obtained for samples of the same core for which spore–pollen, diatom, and preliminary geochemical analyses were made earlier (Blyakharchuk et al., 2017). A total of 54 samples (every 1 cm in the upper 31-cm part and every 2 cm below the 31-cm depth) were used for high-resolution geochemical analysis. A total of 46 elements, including TME, HME, and REE, were analyzed for every sample. It is important to point out that these elements are from the bulk sediment samples which were completely dissolved in HF + HNO_3 + HCl acids by microwave digestion. Therefore, the majority of the elements should come from detritus, mainly from exogenous origins. Their variations probably are mainly due to input change instead of lake chemistry, except for some elements such as alkaline and alkaline earth elements.

Figure 7 plots the variations of selected elements in the core. Among the measured elements, Al, Fe, and Ti are the dominant elements and have high concentrations in the order of mg/g, whereas the other elements are on the orders of mg/kg. Al, Fe, and Ti mainly come from detritus and have a strong positive correlation ($R^2 > 0.9$) with the ash content of the sediment which was determined by loss of ignition at 550°C (Blyakharchuk et al., 2017). Some trace metal and heavy metal elements such as Li, Rb, Th, Nb, Zr, Cr, V, Hf, Sc, and Y have similar patterns as those of Al, Fe, and Ti, indicating that they have the same origins. Together Al, Fe, Ti, Li, Rb, Th, Nb, Zr, Cr, V, Hf, Sc, and Y are considered as lithophilic elements, and their variations are chiefly controlled by detrital input. Furthermore, the REE contents are also strongly correlated with the ash content ($R^2 = 0.88$) (**Figure 8**). Thus, the detrital content of the sediments is the main dominant factor to control the variations of the above-mentioned elements (Dobrovolsky, 1999). Hence, we can classify the geochemical variation of the core as follows:

Zone I: 1,440–1,150 years BP (82–50 cm): high organic (OM) and $CaCO_3$ contents, low ash content, and low TME, HME, and REE contents.

Zone II: 1,150–1,070 years BP (50–40 cm): strongly increased ash content but decreased OM and $CaCO_3$ contents and strongly increased TME, HME, and REE contents.

Zone III: 1,070–850 years BP (40–17 cm): maximum values of ash, lithophilic element, and REE contents, but low OM and $CaCO_3$ contents in the beginning. Then, the lithophilic element and the REE contents gradually decreased.

Zone IV: 850–500 years BP (17–7 cm): the lithophilic element and the REE contents were stable at moderate levels. The sedimentation rate had a significant decrease.

Zone V: 500–50 years BP (7–5 cm): very low sedimentation rate; $CaCO_3$ content increased. Except As and Pb, most elemental concentrations were relatively low.

Zone VI: The last century (5–0 cm): OM and $CaCO_3$ contents increase. Most elemental concentrations are reduced to low values.

The geochemical records shown in **Figures 7**, **8** provide us the lake history under climate influence. During zone I, the lake had relatively high biological productivity as reflected by high OM and $CaCO_3$. The lake was a freshwater lake with a moderate lake level because the organic matter was generally high (28–35%) and the $CaCO_3$ content was only 2–5% in the bulk sediments. With relatively low detritus content, the lake sediments contained low TME, HME, and REE. During zone II, as the surface runoff sharply increased, the OM and the $CaCO_3$ contents rapidly decreased and the ash contents strongly increased, which resulted in strong increases of TME, HME, and REE. During zone III, the surface runoff could be still high. However, as the lake became deeper and larger, sediment loading in the coring site became finer and detritus/OM ratio gradually decreased. The lake level was still high in the beginning of zone IV. Then, as the climate became cooling and drying, the lake input decreased, resulting to lowering of the sedimentation rate during zone IV. The lake had very low sedimentation during zone V due to cold and dry climatic conditions. Until about 100 years ago, the lake started to recover its biological productivity and water input.

Rare earth elements include La, Ce, Pr, Nd, Sm, Eu, Gd, Tb, Dy, Ho, Er, Tm, Tu, Yb, and Lu. Light REEs involve La to Gd, and heavy REEs contain Tb to Lu. Many previous studies have used REE patterns to trace the depositional processes and identify the sediment provenances since they behave conservatively during sediment formation (Prajith et al., 2015; Xu et al., 2017). However, most REE studies of sediment provenances are used in marine environments. For the Manzherok Lake core, the sediment source is relatively simple and the depositional time is relatively short. Therefore, we only use the REE pattern to discuss the sediment feature throughout the core.

Figure 9 shows the REE normalized to North American Shale Composite (NASC) and **Figure 10** reveals the REE normalized to chondrite in different sediment layers. We averaged the patterns

TABLE 2 | Rare earth elements of the Manzherok Lake core samples.

Depth (cm)	Age (a BP)	La	Ce	Pr	Nd	Sm	Eu	Gd	Tb	Dy	Ho	Er	Tm	Yb	Lu	ΣLREE	ΣHREE	ΣLREE/ ΣHREE	ΣREE	δEn	δCe
0–1	−63	20.2	48.5	5.51	21.8	4.60	1.14	4.95	0.72	4.29	0.80	2.28	0.31	2.19	0.30	106.8	10.9	9.8	117.7	1.06	1.07
1–2	−48	20.3	49.5	5.69	22.6	4.84	1.18	5.12	0.74	4.44	0.83	2.36	0.32	2.31	0.32	109.2	11.3	9.7	120.6	1.05	1.07
2–3	−33	20.6	50.2	5.81	23.0	4.86	1.18	5.17	0.75	4.60	0.85	2.39	0.33	2.31	0.33	110.9	11.6	9.6	122.4	1.05	1.06
3–4	−18	21.8	52.8	5.96	23.7	5.05	1.22	5.37	0.78	4.71	0.88	2.53	0.34	2.39	0.34	115.9	12.0	9.7	127.8	1.04	1.08
4–5	−3	27.0	60.5	6.07	24.1	5.16	1.29	5.33	0.75	4.67	0.85	2.55	0.34	2.55	0.33	129.5	12.0	10.8	141.5	1.09	1.10
5–6	203	24.9	55.1	5.57	22.2	4.87	1.13	5.06	0.72	4.14	0.81	2.27	0.31	2.16	0.30	118.9	10.7	11.1	129.6	1.01	1.09
6–7	465	24.7	58.4	5.84	22.6	4.99	1.20	5.24	0.73	4.49	0.85	2.38	0.35	2.40	0.30	123.0	11.5	10.7	134.5	1.04	1.13
7–8	520	24.9	59.4	5.82	22.9	4.98	1.23	5.28	0.74	4.54	0.85	2.41	0.34	2.37	0.35	124.5	11.6	10.7	136.1	1.06	1.15
8–9	574	24.9	60.1	5.90	23.4	4.87	1.24	5.30	0.79	4.61	0.84	2.51	0.33	2.52	0.35	125.8	11.9	10.5	137.7	1.08	1.15
9–10	629	23.9	58.3	5.62	22.2	4.86	1.13	5.16	0.72	4.53	0.83	2.34	0.33	2.46	0.34	121.1	11.6	10.5	132.7	1.00	1.17
10–11	683	23.4	56.9	5.54	22.3	4.74	1.11	5.07	0.69	4.30	0.80	2.33	0.33	2.34	0.33	119.1	11.1	10.7	130.2	1.01	1.16
11–12	724	24.4	58.9	5.81	23.4	4.75	1.18	5.12	0.74	4.42	0.85	2.36	0.35	2.50	0.35	123.6	11.6	10.7	135.1	1.06	1.15
12–13	750	24.5	60.4	5.91	23.0	4.86	1.23	5.29	0.75	4.54	0.84	2.52	0.32	2.64	0.32	125.2	11.9	10.5	137.1	1.08	1.16
13–14	777	23.4	58.2	5.70	21.9	4.82	1.15	5.03	0.73	4.42	0.84	2.39	0.32	2.33	0.31	120.2	11.3	10.6	131.6	1.03	1.17
14–15	803	23.7	58.4	5.62	22.5	4.91	1.19	5.11	0.74	4.37	0.83	2.52	0.34	2.39	0.34	121.4	11.5	10.5	133.0	1.05	1.17
15–16	830	24.6	59.4	5.92	23.0	4.93	1.22	5.07	0.77	4.42	0.84	2.47	0.35	2.32	0.34	124.2	11.5	10.8	135.7	1.08	1.14
16–17	848	23.7	57.1	5.50	22.0	4.92	1.09	5.00	0.73	4.25	0.81	2.36	0.32	2.39	0.35	119.3	11.2	10.6	130.5	0.98	1.16
17–18	859	24.0	59.6	5.76	23.2	5.08	1.18	5.27	0.74	4.56	0.85	2.46	0.33	2.41	0.34	124.2	11.7	10.6	135.8	1.01	1.18
18–19	871	25.7	62.6	6.16	24.6	5.27	1.28	5.50	0.81	4.82	0.90	2.67	0.36	2.39	0.35	131.0	12.3	10.6	143.3	1.06	1.15
19–20	882	26.5	63.7	6.40	25.1	5.78	1.35	5.68	0.80	4.91	0.93	2.75	0.38	2.62	0.36	134.5	12.7	10.5	147.2	1.05	1.13
20–21	893	25.1	60.7	5.92	23.6	4.86	1.20	5.35	0.76	4.57	0.85	2.46	0.35	2.46	0.33	126.7	11.8	10.8	138.5	1.05	1.16
21–22	902	24.7	60.9	5.97	23.9	5.05	1.28	5.28	0.75	4.80	0.87	2.61	0.36	2.57	0.36	127.0	12.3	10.3	139.3	1.10	1.16
22–23	909	25.1	61.2	6.08	24.0	5.18	1.25	5.45	0.78	4.69	0.87	2.59	0.36	2.54	0.37	128.3	12.2	10.5	140.5	1.04	1.15
23–24	915	28.1	60.4	5.98	23.2	4.96	1.24	5.43	0.76	4.81	0.87	2.60	0.36	2.51	0.35	129.3	12.3	10.5	141.5	1.06	1.08
24–25	922	25.4	60.4	5.94	23.5	5.15	1.19	5.19	0.76	4.55	0.84	2.55	0.37	2.42	0.35	126.8	11.8	10.7	138.6	1.02	1.14
25–26	929	24.8	59.1	5.83	23.0	4.98	1.24	5.20	0.75	4.57	0.88	2.58	0.37	2.44	0.35	124.1	11.9	10.4	136.1	1.08	1.14
26–27	938	24.8	59.2	5.75	23.2	5.02	1.23	5.28	0.76	4.66	0.83	2.52	0.37	2.49	0.35	124.4	12.0	10.4	136.4	1.06	1.15
27–28	950	26.6	61.8	6.02	24.0	5.05	1.25	5.29	0.77	4.53	0.88	2.65	0.36	2.58	0.35	129.9	12.1	10.7	142.0	1.07	1.13
28–29	962	28.2	61.1	5.99	23.3	4.92	1.17	5.26	0.77	4.75	0.88	2.52	0.35	2.69	0.37	130.0	12.3	10.5	142.3	1.02	1.09
29–30	974	24.0	61.1	5.92	23.8	5.26	1.31	5.24	0.82	4.79	0.89	2.66	0.38	2.67	0.39	126.7	12.6	10.1	139.3	1.11	1.19
30–31	986	24.9	63.2	6.16	24.7	5.16	1.29	5.43	0.78	4.97	0.93	2.75	0.38	2.52	0.36	130.8	12.7	10.3	143.5	1.09	1.18
32–33	1006	25.7	63.8	6.34	25.2	5.43	1.33	5.33	0.83	4.88	0.93	2.81	0.38	2.74	0.39	133.1	13.0	10.3	146.1	1.10	1.16
34–35	1025	26.9	65.0	6.60	26.2	5.54	1.37	5.76	0.89	5.21	0.99	2.79	0.40	2.80	0.38	137.4	13.5	10.2	150.8	1.08	1.13
36–37	1043	27.8	66.6	7.08	27.3	5.98	1.41	6.23	0.90	5.32	1.00	2.99	0.43	2.97	0.41	142.3	14.0	10.1	156.4	1.03	1.10
38–39	1060	29.1	68.7	7.27	28.2	6.12	1.38	6.23	0.93	5.39	1.02	3.24	0.41	2.94	0.41	147.0	14.4	10.2	161.4	0.99	1.10
41–42	1086	23.9	57.1	5.77	23.3	5.04	1.28	5.34	0.74	4.77	0.89	2.67	0.34	2.59	0.36	121.7	12.4	9.8	134.0	1.09	1.13
43–44	1103	20.5	53.9	5.35	21.5	4.64	1.09	4.67	0.70	4.40	0.79	2.38	0.33	2.36	0.32	111.7	11.3	9.9	123.0	1.04	1.20
45–46	1120	17.9	48.4	4.68	18.9	4.02	1.00	4.35	0.62	3.75	0.70	2.05	0.28	1.95	0.27	99.3	9.6	10.3	108.9	1.06	1.23
47–48	1137	15.9	43.3	4.15	16.5	3.66	0.88	3.84	0.57	3.24	0.61	1.86	0.24	1.79	0.22	88.2	8.5	10.3	96.8	1.04	1.24
49–50	1155	14.9	40.9	3.87	15.2	3.25	0.80	3.45	0.52	3.14	0.56	1.68	0.23	1.58	0.22	82.3	7.9	10.4	90.3	1.06	1.25
51–52	1173	13.7	37.8	3.48	13.7	3.04	0.74	3.30	0.46	2.69	0.54	1.47	0.22	1.47	0.20	75.8	7.1	10.8	82.9	1.04	1.27
53–54	1193	13.6	38.0	3.44	14.1	3.13	0.73	3.09	0.44	2.76	0.50	1.48	0.21	1.41	0.21	76.1	7.0	10.8	83.1	1.03	1.28
55–56	1212	13.7	37.0	3.46	13.8	2.91	0.76	3.20	0.46	2.83	0.52	1.51	0.21	1.44	0.19	74.9	7.2	10.4	82.0	1.11	1.25
57–58	1231	13.9	37.7	3.55	14.4	3.01	0.78	3.34	0.46	2.80	0.54	1.52	0.22	1.52	0.20	76.6	7.2	10.6	83.8	1.09	1.25
59–60	1251	13.4	37.1	3.52	13.7	2.97	0.72	3.14	0.44	2.76	0.50	1.49	0.21	1.36	0.22	74.5	7.0	10.7	81.5	1.04	1.25
61–62	1269	13.4	37.2	3.50	14.0	2.99	0.76	3.40	0.45	2.76	0.55	1.57	0.21	1.50	0.20	75.3	7.3	10.4	82.6	1.06	1.26
63–64	1285	14.3	38.9	3.71	14.7	3.16	0.77	3.30	0.48	2.95	0.56	1.50	0.22	1.54	0.21	78.8	7.5	10.6	86.3	1.05	1.24
65–66	1301	15.4	40.9	3.88	15.3	3.32	0.84	3.48	0.51	3.06	0.57	1.63	0.23	1.64	0.23	83.1	7.9	10.6	91.0	1.09	1.23
68–69	1320	14.7	39.6	3.75	15.4	3.19	0.79	3.15	0.49	3.01	0.53	1.58	0.24	1.49	0.21	80.5	7.5	10.7	88.0	1.10	1.24
70–71	1333	19.0	40.1	4.03	16.0	3.40	0.85	3.56	0.51	3.12	0.59	1.67	0.22	1.62	0.22	87.0	8.0	10.9	94.9	1.08	1.06

(Continued)

TABLE 2 | Continued

Depth (cm)	Age (a BP)	La	Ce	Pr	Nd	Sm	Eu	Gd	Tb	Dy	Ho	Er	Tm	Yb	Lu	SLREE	SHREE	SLREE/ SHREE	SREE	dEn	dCe
72–73	1348	13.8	38.3	3.61	14.9	3.06	0.74	3.25	0.47	2.95	0.57	1.57	0.21	1.48	0.22	77.8	7.5	10.4	85.2	1.05	1.26
73–74	1357	13.8	38.3	3.49	14.2	3.10	0.76	3.28	0.49	2.83	0.53	1.46	0.21	1.50	0.20	76.9	7.2	10.7	84.1	1.06	1.28
75–76	1373	14.8	39.2	3.82	15.3	3.33	0.77	3.34	0.47	2.98	0.55	1.56	0.22	1.55	0.23	80.5	7.6	10.7	88.0	1.02	1.21
77–78	1390	14.0	37.5	3.62	14.3	3.31	0.79	3.32	0.48	2.98	0.53	1.58	0.22	1.53	0.20	76.8	7.5	10.2	84.4	1.06	1.22
79–80	1406	14.1	38.5	3.74	14.7	3.27	0.78	3.39	0.49	3.15	0.56	1.61	0.21	1.60	0.21	78.4	7.8	10.0	86.2	1.04	1.23
81–82	1421	14.3	38.0	3.61	14.8	3.22	0.79	3.53	0.50	2.93	0.53	1.56	0.20	1.47	0.23	78.2	7.4	10.5	85.6	1.03	1.23
Average		21.3	52.5	5.20	20.6	4.44	1.08	4.66	0.67	4.08	0.76	2.22	0.31	2.17	0.30	109.8	10.5	10.4	120.3	1.05	1.17
St. Deviation	5.2	10.3	1.12	4.3	0.93	0.22	0.95	0.14	0.83	0.16	0.49	0.07	0.48	0.07	22.8	2.2	0.3	25.0	0.03	0.06	

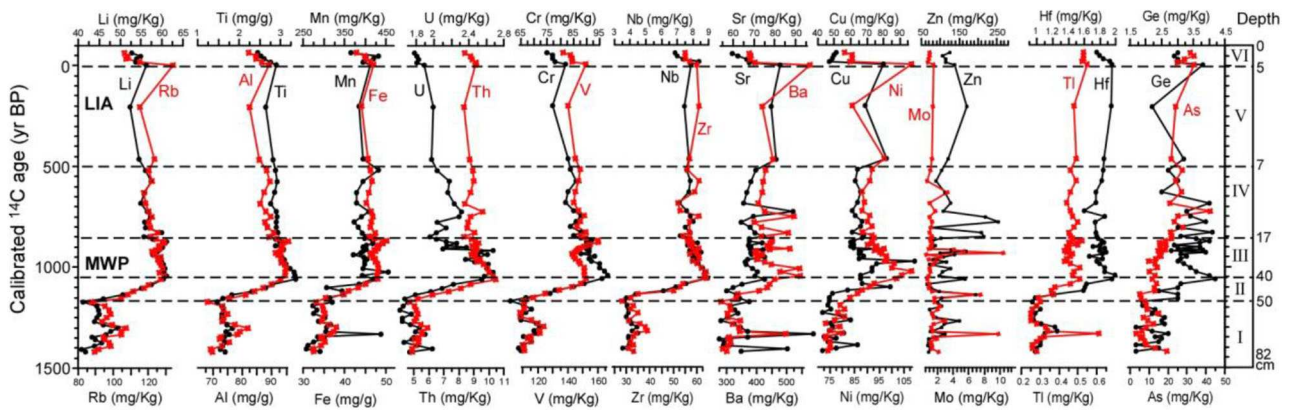

FIGURE 7 | Selected elemental concentrations in the lake sediments throughout the Manzherok Lake sediment core. Note that the units for Al, Ti, and Fe are in mg/g, whereas the rest of the elements are in mg/kg.

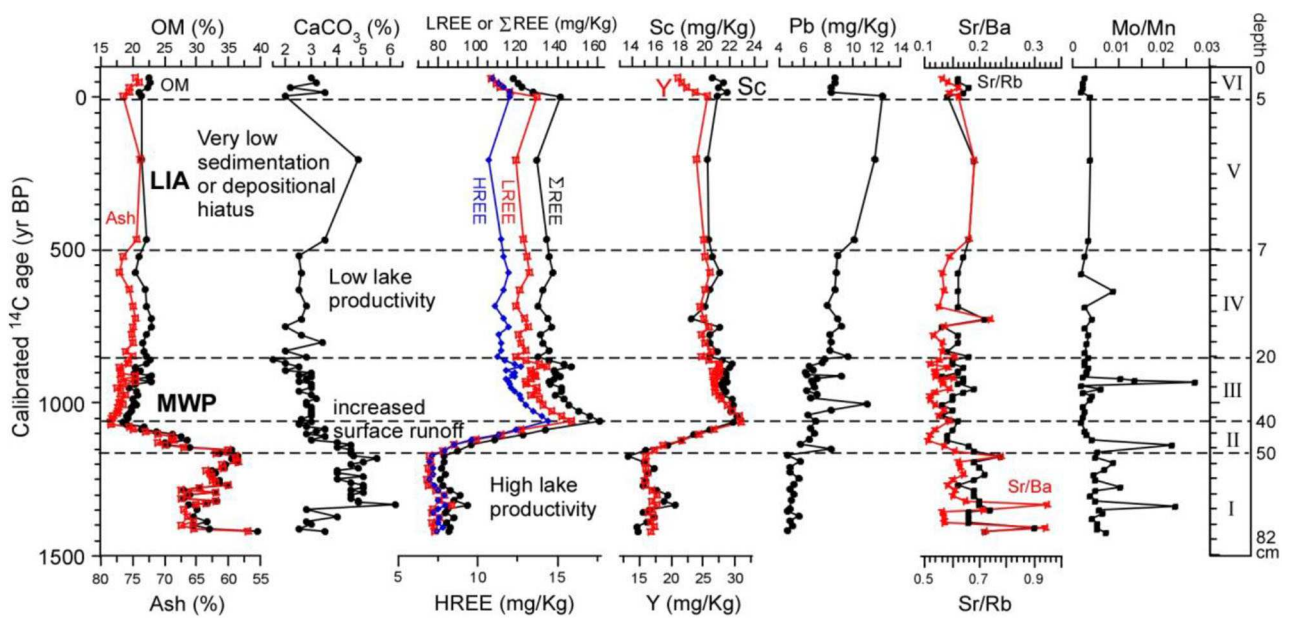

FIGURE 8 | Classification of the geochemical zones in the Manzherok Lake sediment core.

of 51–82 cm as their ratios in the different layers of this zone are quite similar. In the two figures, although the patterns are all similar, the values of the normalized ratios can be grouped into three categories: (1) 51–82 cm, (2) above 29–33-cm layer, and (3) between 34–35-cm layer and 49–50-cm layer. In the first category which is corresponding to zone I, both NASC and chondrite normalized ratios are the lowest, and the ratios of Ho, Er, Tm, Yb, and Lu to NASC are the same (**Figure 9**). The feature of the first category can be considered as the organic-rich sediments with a relatively constant input, which can be regarded as an end-member of the mixed lake sediments with another end-member from the surface runoff. In the second category, the values of both NASC and chondrite normalized patterns increased from the 49–50-cm layer to the 38–39-cm layer and then slightly decreased to the 34–35-cm layer (**Figures 9, 10**). In principle, the REEs in the lake sediments are mainly from detrital input carried by surface runoff. When the detrital input increases with the surface runoff under wet climates, the REE contents should increase. The patterns at different layers are basically the same, indicating that the detrital source, which is from the surrounding area of the lake, remains relatively constant. The variations in the NASC and chondrite normalized ratios shown in **Figures 9, 10** depend on the percentage of the input detritus in the lake sediments. The higher ratios reflect a higher percentage of the input detritus, which is confirmed by the increasing ash content from the 49–50-cm layer to 38–39-cm layer. Therefore, the changes in the geochemical proxies during the depositional period of 50–40 cm in the lake core (zone II, 1,150–1,070 years BP) reflected strongly the increased detrital input due to the enhanced surface runoff under wet climates. The third category shows that the patterns and the ratios are similar, especially for the chondrite normalized ratios (**Figure 10**). This means that the amount of detrital input to the lake sediments at the coring site from the surface runoff reduced after deposition at 33-cm depth (1,005 years BP). Such a situation could be caused by both increased lake level, so that it was difficult for the sediments from the surface runoff to reach the depo-center where the core was retrieved, and reduced surface runoff.

The variation trends of As, Cd (not shown), and Pb are different from those of lithophilic elements (**Figures 7, 8**). Except

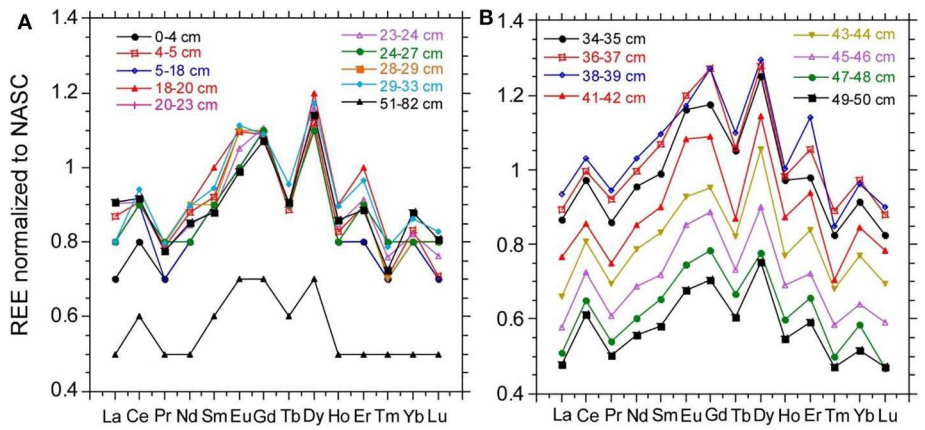

FIGURE 9 | (A,B) Rare earth element patterns normalized to chondrite at different depths in the Manzherok Lake sediment core.

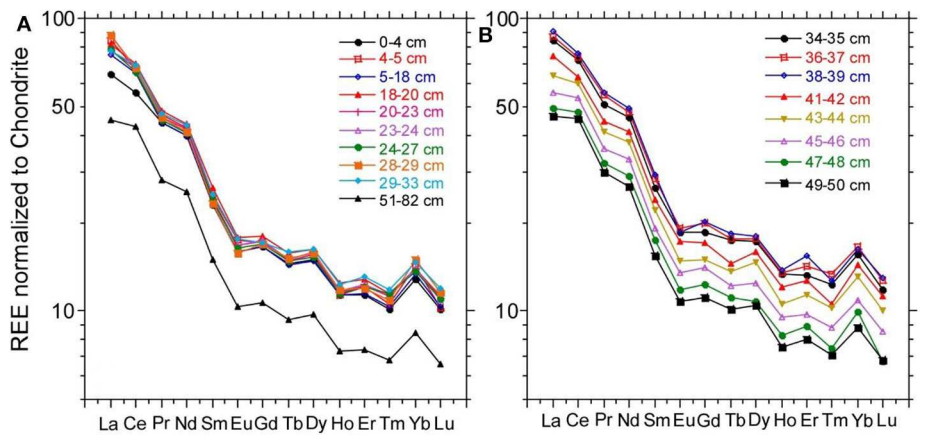

FIGURE 10 | (A,B) Rare earth element patterns normalized to North American shale composition at different depths in the Manzherok Lake sediment core.

at the surface 5 cm, these elements have a general increasing trend from the bottom to the upper section. **Figure 11** exhibits that those toxic elements have some positive correlations (R^2 = 0.39 for Pb vs. Cd and R^2 = 0.46 for Pb vs. As). Normally, these elements have low concentration in the natural background so that their origins should not come from detrital materials. The accumulation of these elements in the lake sediments may be related to the metabolic processes of living organisms and anthropogenic activities.

Sr, Ba, and Rb are IIA elements in the periodic table and have similar chemical characteristics. However, Sr is more influenced by lake water chemistry, whereas Ba and Rb are mainly from detritus. **Figure 11** shows the significant correlation ($R^2 = 0.735$) between Rb and Ba, but weak or no correlation (R^2 = 0.15) between Rb and Sr. Using the Sr/Ba and the Sr/Rb ratios, one may eliminate detrital influence so that the effect of lake chemistry can be seen. Sr prefers to co-precipitate with carbonate and favors high alkalinity and lake productivity. The variations of Sr/Ba and Sr/Rb in the core show peaks at 1,410, 1,335, 1,175, and 725 year BP, which also correspond to peaks in $CaCO_3$ (**Figure 8**). During those periods, the lake had relatively high productivity and alkalinity. A slight increase in Sr/Ba, Sr/Rb, and $CaCO_3$ during LIA might not reflect an increase in lake productivity. Under dry climatic condition during LIA, the lake level or volume decreased so that the concentrations of Ca^{2+} and CO_3^{2-} in the lake might be enhanced to raise alkalinity and pH, resulting in carbonate precipitation.

The Mo/Mn ratio is correlated well with the anoxic environment (Kalugin et al., 2014), whereas the Mn-enriched layer marks a long-term pause of sedimentation in the oxidized systems. In **Figure 8**, the Mo/Mn peaks appeared at 1,335, 1,270, 1,140, 930, and 630 years BP, indicating the anoxic conditions in the lake, which reflected high lake productivity under relatively warm and moist conditions on decadal time scales in the study area.

High Sr/Ba, Sr/Rb, Mo/Mn, and $CaCO_3$ appeared at around 1,335, 1,140, and 930 years BP, reflecting high lake productivity. These periods also coincide with the mass bloom of algae and cyanobacteria *Anabaena*. Thus, the geochemical proxies and the biological proxies agree with each other, confirming the observations.

BIOLOGICAL AND GEOCHEMICAL PROXIES IN THE MANZHEROK LAKE CORE AS INDICATORS OF CLIMATIC AND ENVIRONMENTAL CHANGE OVER THE PAST 1,500 YEARS

The biological and the geochemical records of the Manzherok Lake core with the new chronology provide us with details on lake history and vegetation change under climate regimes and human impacts since 1,440 years BP. In **Figure 12**, we summarize the major geochemical proxies in the core and compare them with the total solar irradiance (Bard et al., 2000; Steinhilber et al., 2009). The OM, ash, and $CaCO_3$ contents reflect the sediment feature which briefly dominate the lake geochemical and productivity signals. The concentrations of total REE, Al, and Ti represent detrital inputs. Sr/Ba and Sr/Rb can be considered as indicators of lake alkalinity and productivity. Mo/Mn may illustrate anoxic conditions. The shortage of this record is that the sedimentation rate was too low during the Little Ice Age so that the interpretation for this period is brief. In the following, we shall describe the record for each lake and climate stages one by one:

1,440–1,150 years BP (zone I for geochemical proxies and zone 1 for pollen records): This period is prior to the Medieval Warm Period. During this period, the lake had a moderately high level, with relatively high productivity and alkalinity under a frequently anoxic condition, which was shown by high organic matter and carbonate contents, peaks of Sr/Ba, Sr/Rb, and Mo/Mn, and mass bloom of algae and cyanobacteria *Anabaena*. Vegetation in the area was a phase of birch forest–steppe with a high abundance

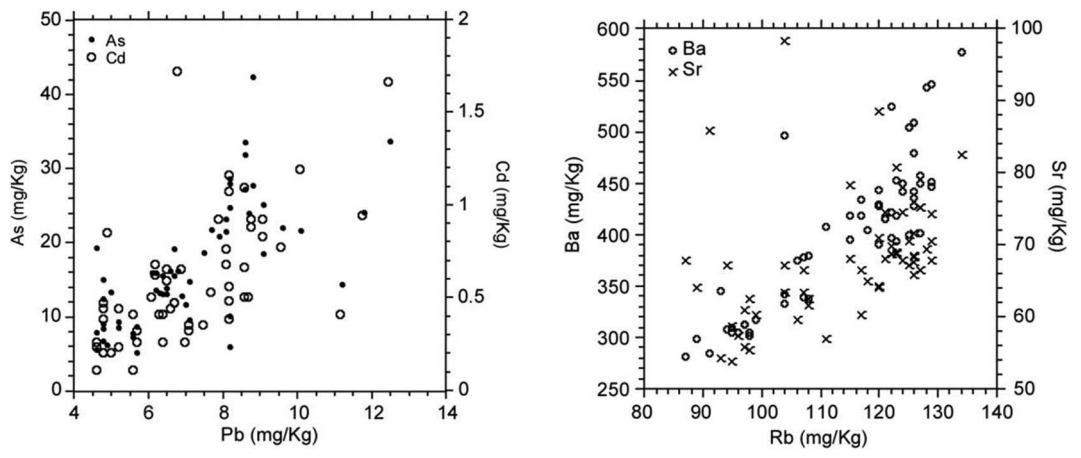

FIGURE 11 | Left: correlations among toxic elements of Pb, Cd, and As. **Right**: relationships among Sr, Ba, and Rb.

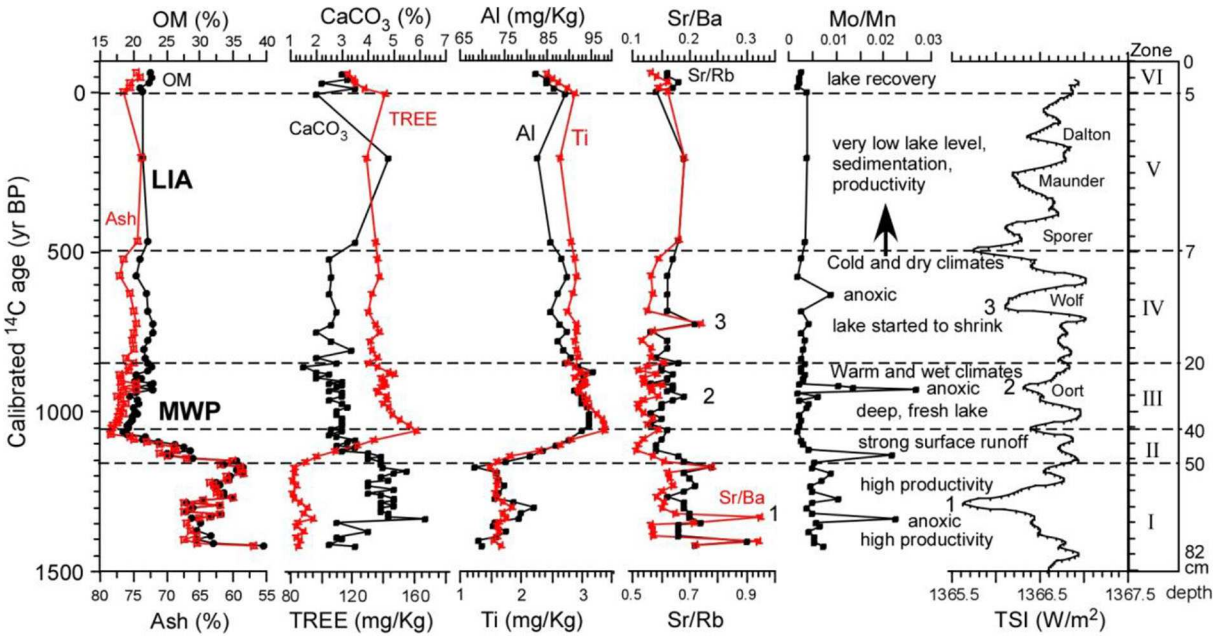

FIGURE 12 | Comparison of important geochemical indices in the Manzherok Lake core with the total solar irradiance (TSI). The TSI curve is a five-point running average of the 5-years resolution TSI data from Steinhilber et al. (2009). Numerical numbers 1, 2, and 3 for the Sr/Ba and the TSI plots denote their correlations.

of *Nymphaea* and *B. pendula* and relatively low *P. sylvestris*. The climatic conditions were moderately warm and wet. Surface runoff to the lake was not strong so that detrital input from the surrounding lake was low. Decadal scales of warm but dry episodes appeared at 1,335, 1,270, and 1,140 years BP.

1,150–1,070 years BP (zone II for geochemical proxies and zone 2 for pollen records): Manzherok Lake had a sudden change due to wet climates. The surface runoff strongly increased and brought high sediment input to the lake, shown by strongly decreased OM and $CaCO_3$ and strongly increased ash content, lithophilic elements, and REE. The lake level increased so that lake productivity and alkalinity decreased (Sr/Ba and Sr/Rb strongly dropped) and the anoxic condition (Mo/Mn peak) was further enhanced. The REE concentrations continuously increased and reached a maximum at 1,070 years BP. The vegetation in the area became transitional phase from birch forest–steppe to birch and pine forests. The abundance of *B. pendula* sharply decreased and *Nymphaea* disappeared, while *P. sylvestris* increased. In the lake, algae and *Anabaena* were abundant, reflecting that the lake was still productive. The wet and warm climates marked the onset of MWP.

Anthropogenic influence on the landscape began. Approximately from 1,130 years BP or slightly earlier, one can see permanent findings of the pollen of cultivated plant *Triticum* supplemented by the pollen of field weeds. Simultaneously, we count abundant microcharcoal in pollen slides. It is evidence of spreading of fire-cutting agriculture on the western piedmonts of the Altai Mountains. According to these evidences, fire-cutting agriculture began to spread here a few centuries before the Russian colonization. It is worth to mention that human activity could cause the loosening of the earth surface, which might introduce more sediment input to the lake.

1,070–850 years BP (zone III for geochemical proxies and zone 3 for pollen records): This interval had warm and wet climates corresponding to MWP. Manzherok Lake was the largest and deepest during this period over the past 1,500 years. Due to the deepening of the lake throughout high and frequent surface runoffs in the previous stage, the sediments at the depo-center, where the core was retrieved, contained less detritus as shown by reduced contents of ash, REE, and lithophilic elements. In the early half of this period, the lake was very fresh and had low productivity (very low Sr/Ba and Sr/Rb). However, during the late half of the period, the lake productivity and the alkalinity (increased Sr/Ba, Sr/Rb, and OM content) increased, and the anoxic condition (highest Mo/Mn peak) at the bottom of the lake became very strong. The vegetation in the area was a phase of birch and pine forests during this period, reflecting warm and moist conditions. The abundance of *P. sylvestris* reached its maximum (ca. 40%), *B. pendula* dropped to its minimum (∼20%), and *Nymphaea* disappeared, showing the dynamic change of the local vegetation. The enhanced *Bryales*/algae and *anabaena* abundances and the REE and lithophilic elements before the end of this stage indicate that the lake started to drop its level (**Figure 8**). The humidity index, as reconstructed by the pollen data using the equation of Wang et al. (2010), provided a semi-quantitative moisture change (Blyakharchuk et al., 2017), showing the highest humidity at around 950–900 years BP (**Figure 6**). After 900 years BP, the climate became dry.

Owing to the deep and anoxic conditions of Manzherok Lake during MWP, the submerged plants and algae would uptake dissolved CO_2 which could not fully exchange with the atmospheric CO_2. Because the dissolved CO_2 contained partial CO_2 which was decomposed from old organic matter in the deeper sediments, its ^{14}C had an initial age. Therefore, even though many samples from this interval were gone through ABA treatment, their ages are still older than their true ages because the ABA treatment could not remove the old carbon influence caused by the uptake of dissolved CO_2.

The anthropogenic influence during this period became more significant as shown by the accumulation of toxic elements including Pb, As, and Cd. Metal elements such as Ni, Cu, and Zn commonly exit in the copper ore. The joint finding of Zn and Cu in the bones of people was considered as an indicator of their involvement in the metallurgical process (Aleksandrovskaya and Aleksandrovsky, 2007). The same authors pointed out that during the smelting of copper from copper and polymetallic ores and even during the remelting of copper objects, Zn could evaporate together with metallurgical gases. When the metallurgical gases contacted with cold air, Zn could condense and fall on the ground. The maximum Cu concentration appeared at 980 years BP, probably reflected as ancient smelting in the local area.

850–500 years BP (zone IV for geochemical proxies and lower zone 4 for pollen records): The vegetation after 850 years BP was determined as a phase of pine–birch forest–steppe. The lake sedimentation rate began to drop rapidly due to drying and cooling climatic conditions. The humidity index based on the pollen data dropped significantly and was kept at a low level (**Figure 6**). The concentrations of REEs and lithophilic elements in this interval was kept relatively constant at lower values than those in zone III, indicating a lower detrital input corresponding to reduced sedimentation rate under a dry climate. The lake level declined gradually so that carbonate precipitation slightly increased at 800 years BP (**Figure 12**). A slight increase in REE and lithophilic elements at 750 years BP probably indicated that the lake reached a low steady level with moderate productivity. The lake enhanced its alkalinity at 725 years BP as reflected by the peaks of Sr/Ba and Sr/Rb due to the further shrinking of the lake volume. As the lake volume shrank, its nutrient concentration increased so that the lake productivity also slightly increased, as shown by the enhanced abundance of algae and *Anabaena* between 700 and 600 years BP (**Figure 6**). A weak but apparent anoxic condition of the lake occurred at around 630 years BP. After 600 years BP, the climatic condition in the study area entered into cold LIA.

According to history record, the first Mongolian invasion to Siberia was 1,207 CE (743 years BP). The time period that Mongolia conquered the Altai region was 1,236–1,242 years CE (714–708 years BP). Thus, the two Zn peaks, together with a slight increase in the Cu and the Ba contents at 850–830 and 770–750 years BP, in our record might reflect the metallurgical practice of local human tribes who lived on the western piedmonts of the Altai Mountains in XII century CE. The humidity index based on the pollen record and the geochemical proxies of the Manzherok core illustrate that the climate was moist during the beginning of the Mongolian invasion, although the climate during this period was not as wet as that during MWP. The Mongol Empire can be divided in two parts: 1,206 CE (744 years BP) to 1,270 CE (680 years BP) before the Yuan Dynasty and 1,271 CE (679 years BP) to 1,368 CE (582 years BP) of the Yuan Dynasty. The first part, especially during the Chenghis Khan reign, was mainly active in the north regions including Altai, Siberia, whereas the second part was mainly active in Mongolia and northern China. According to the Manzherok Lake record, the climate in the study area began cooling and drying at around 750 years BP and became much worse after 600 years BP. The climatic conditions certainly affected human activity in the study area.

500–50 years BP (zone V for geochemical proxies and middle zone 4 for pollen records): The lake depositional record in this interval corresponds to LIA. The sedimentation rate was very low and often had depositional hiatuses due to cold and dry conditions during this period. For only the 2-cm sediments in this interval, the pollen and geochemical data were not good enough to interpret the detailed lake history. Nevertheless, the extreme sedimentation was attributed not only to low surface runoff under dry climates but also to longer frozen time under cold conditions.

After 1,950 CE (zone VI for geochemical proxies and upper zone 4 for pollen records): The top 5-cm sediments containing nuclear bomb ^{14}C indicate that they were deposited after 1,950 CE. In the 5-cm layer, one can still see clear trends of increasing OM, decreasing ash content, and declining concentrations of REE and lithophilic elements. These trends reflect the recovery of lake productivity and deposition in the current warming centenary.

The above description of Manzherok Lake history and the local climatic conditions over the past 1,500 years refine our findings in Blyakharchuk et al. (2017). The detailed pollen data and the geochemical proxies consistently illustrate the climate changes well. We have compared this record with the pollen and geochemical records from Teletskoye Lake which is 100 km east during the past 1,000 years (Andreev et al., 2007; Kalugin et al., 2007). The climate reconstruction-based pollen record (**Figure 6**) in Teletskoye Lake during the last 1,000 years (Andreev et al., 2007) are summarized as follows: (1) humid climate of late MWP 1,000–880 years BP and dry climate 880–750 years BP, (2) humid climate 750–550 years BP, and (3) dry climate of LIA 520–110 years BP. Our Manzherok Lake record agrees well with the above-mentioned climate reconstructions. We have also found a good correlation of Sr/Rb index between the Manzherok Lake record and the Teletskoye Lake record (Kalugin et al., 2007). However, we should mention that Manzherok Lake is much smaller and shallower than Teletskoye Lake so that the sedimentations in the two lakes are different. In the Teletskoye Lake sediments, annual laminations can be found, whereas the Manzherok Lake sediments do not show laminations; they instead contain much more plant remains (OM > 20%). In addition, because Manzherok Lake is small and shallow, it has a longer frozen time than Teletskoye Lake. Hence, the sedimentary hiatus during LIA did not occur in Teletskoye Lake. Under such circumstances, Manzherok Lake is more

sensitive to climate change than Teletskoye Lake in terms of geochemical proxies.

In **Figure 12**, a comparison of the Manzherok Lake record to the TSI record shows good correlations not only on the long-term major changes of the lake but also on decadal events corresponding to the climate changes. In general, a large, deep, and fresh lake with high sedimentation exists under warm and wet climates such as MWP. A small and shallow lake stage with low sedimentation appears under cold and dry climates such as LIA. During a long relatively warm and wet period, a TSI minimum resulting in a dry episode would lead to lake shrinkage that will cause a rise in lake alkalinity and productivity so that increased Sr/Ba and Sr/Rb could result. In **Figure 12**, numbers 1, 2, and 3 denote the correlations between Sr/Ba (and Sr/Rb) and TSI minimum within age uncertainties. Thus, we conclude that the climate of the study area is strongly influenced by total solar irradiance, with higher TSI resulting in warmer and wetter conditions. Since the westerly and the polar easterly are the two major moisture jet streams to the area, when lower TSI causes a stronger Siberian High, the latter probably pushes both the westerly and the polar front away from the study area, resulting in arid climates. The situation is reversed *vice versa*.

CONCLUSIONS

The high-resolution multiproxy analyses including pollen, diatom, contents of total organic carbon, carbonate and ash, concentrations of trace metal elements, heavy metal elements, and rare earth elements in an 82-cm sediment core from Manzherok Lake reveal detailed changes in vegetation and climate in the western foothills of the Altai Mountains over the past 1,500 years. A total of 48 AMS ^{14}C dates combined with ^{210}Pb dating indicate that the lake had very low sedimentation (only ∼2 cm) during LIA due to cold and dry climates. There are many ABA-treated samples that show old carbon influence on their ^{14}C ages because ABA treatment cannot remove organic compounds which used old dissolved CO_2 in the lake at high and anoxic stages. High-resolution ^{14}C dating on such lake cores should apply for solving such a problem.

Vegetation development in this region can be classified as (1) phase of birch forest–steppe during 1,440–1,150 years BP, (2) transitional phase from birch forest–steppe to birch and pine forests dated 1,150–1,070 years BP, (3) phase of birch and pine forests during 1,070–850 years BP, and (4) phase of pine–birch forest–steppe after 850 years BP. Aquatic pollen species such as algae, *Nimphae* cell, and cianobacterium *Anabaena* provide details on the changes in the lake ecosystem.

Changes in the contents of organic matter, ash, and $CaCO_3$ (dominant sediment feature), concentrations of lithophilic and REE elements (detrital inputs), Sr/Ba and Sr/Rb (indicators of lake alkalinity and productivity), and Mo/Mn (anoxic conditions) identify six stages in the lake history corresponding to the climate changes: (1) 1,440–1,150 years BP. The lake was moderately deep with high productivity under relatively warm and wet climates: (2) 1,150–1,070 years BP. Strong surface runoff into the lake resulting from wet climates marked the onset of MWP: (3) 1,070–850 years BP. Large, deep, and fresh lake exited due to warm and wet climates during MWP. Decomposed old organic matter in the anoxic bottom caused old carbon influence on the ^{14}C ages: (4) 850–500 years BP. In the early stage, the lake dropped its level slowly until about 700 years BP. Then, the lake shrank its size quickly corresponding to the cooling and drying climates: (5) 500–50 years BP. Small and shallow lake with very low sediment deposition corresponded to cold and dry LIA. (6) The lake has been recovered during the current warming century.

The Manzherok record compares well with the total solar irradiance record, indicating that changes in TSI is an important factor to influence climate in the Altai Mountains. The Siberian High became strong during the TSI minima. Consequently, the westerly and the polar front would be pushed away from this region, resulting in arid climates.

The pollen and charcoal records and the metal elemental concentrations indicate that fire-cutting agriculture began to spread in the Altai Mountains several centuries before the Russian colonization, and the metallurgical practice of local human tribes who lived on the western piedmonts of the Altai Mountains took place in XII century AD before the Mongolian invasion.

DATA AVAILABILITY STATEMENT

The raw data supporting the conclusions of this article will be made available by the authors, without undue reservation, to any qualified researcher.

AUTHOR CONTRIBUTIONS

TB and H-CL designed Research Topic and wrote the manuscript. H-CL and S-CK performed ^{14}C dating. TB and VU conducted pollen and geochemical analyses. All authors contributed to the article and approved the submitted version.

FUNDING

This study was carried out in the framework of the state budget theme of IMCES SB RAS No. AAAAA-A16-116041356666-6 and with the support of the RFBR grants 13-04-00984a, 14-04-10054/k, 52020/MHT_a, and 20-55-53015/20. Funding support to H-CL in Taiwan include MOST 106-2923-M-002—002 -MY3, MOST 106-2116-M-002-012, and MOST 107-2116-M-002-005.

ACKNOWLEDGMENTS

We are thankful to T. S. Papina and P. A. Blyakharchuk for assistance in the field drilling of the Manzherok Lake sediments.

REFERENCES

Aleksandrovskaya, E. I., and Aleksandrovsky, A. L. (2007). *Anthropochemistry. Tutorial*. Moscow: "Class-Mb" Press.

Andreev, A. A., Pierau, R., Kalugin, I. A., Daryin, A. V., Smolyaninova, L. G., and Diekmann, B. (2007). Environmental changes in the northern Altai during the last millennium documented in Lake Teletskoye pollen record. *Quat. Res.* 67, 394–399. doi: 10.1016/j.yqres.2006.11.004

Appleby, P. G. (2001). "Chronostratigraphic techniques in recent sediments," in *Tracking Environmental Change Using Lake Sediments 1,* eds W. M. Last and J. P. Smol (Nedherlands: Springer E-Publishing Inc.), 171–203. doi: 10.1007/0-306-47669-X_9

Bard, E., Raisbeck, G., Yiou, F., and Jouzel, J. (2000). Solar irradiance during the last 1200 years based on cosmogenic nuclides. *TELLUS B* 52, 985–992. doi: 10.3402/tellusb.v52i3.17080

Baskaran, M., Nix, J., Kuyper, C., and Karunakara, N. (2014). Problems with the dating of sediment core using excess 210Pb in a freshwater system impacted by large scale watershed changes. *J. Environ. Radioact.* 138, 355–363. doi: 10.1016/j.jenvrad.2014.07.006

Benoit, G., and Hemond, H. F. (1991). Evidence for diffusive redistribution of ^{210}Pb in lake sediments. *Geochim. Cosmochim. Acta* 55, 1963–1975. doi: 10.1016/0016-7037(91)90036-5

Blaauw, M., and Christen, J. A. (2011). Flexible paleoclimate age-depth models using an autoregressive gamma process. *Bayesian Anal.* 6, 457–474. doi: 10.1214/ba/1339616472

Blyakharchuk, T. A., Eirikh, A., Mitrofanova, E., Li, H. -C., and Su-Chen Kang, S. -C. (2017). High resolution palaeoecological records for climatic and environmental changes during last 1500 years from Manzherok Lake, western foothills of the Altai Mountains, Russia. *Quat. Int.* 447, 59–74. doi: 10.1016/j.quaint.2017.06.014

Bobrov, V. A. (2007). "Estimation of the flows of mineral matter from the atmosphere in the late Holocene. Problems of geochemistry of endogenous processes in the environment: materials of all russian scientific," in *Conf. Publishing house of the Institute of Geography SB RAS*, Irkutsk, v.1, 128–132. (In Russian).

Bobrov, V. A., Bogush, A. A., and Leonova, P. F. (2011). Abnormal manifestations of zinc and copper concentrations in the peat bog of the upper marsh of the southern urals. *Rep. Rus. Acad. Sci.* 439, 784–788. (In Russian). doi: 10.1134/S1028334X11080228

Bobrov, V. A., Leonova, G. A., Strakhovenko, V. D., and Krasnobaev, V. A. (2007). Geochemical role of living matter (plankton, macrophytes) in the formation of organogenic deposits of some lakes in siberia. ecology of biosystems: problems of study, indication and forecasting: *Proceedings of the Intern. Scientific. -Pract. Conf.*, 20-25 Aug. (2007). Publishing house of ASU, Astrakhan, v. 1., 17-24. (In Russian).

Boyarkina, A. P., Baikovsky, V. V., and Vasiliev, N. V. (1993). *Aerosols in Natural Plates in Siberia*. TSU Press, Tomsk. (In Russian).

Brock, F., Higham, T., Ditchfield, P., and Ramsey, C. B. (2010). Current pretreatment methods for AMS radiocarbon dating at the Oxford radiocarbon accelerator unit (ORAU). *Radiocarbon* 52, 103–112. doi: 10.1017/S0033822200045069

Cooke, C. A., Abbott, M. B., Wolfe, A. P., John, L., and Kittleson, J. L. (2007). A millennium of metallurgy recorded by lake sediments from morococha, peruvian andes. *Environ. Sci. Technol.* 41, 3469–3474. doi: 10.1021/es062930+

Darin, A., Kalugin, I., Tretiakov, G., Maksimov, M., Rogozin, D., Zykov, V., (2014). "Reconstruction of the lake Dhira level diring the last 1500 years according to microstratigraphic studies bottom sediments," in *Paleolimnology of Northern Eurasia. Proceedings of the International Conference*, eds D. Subetto, T. Regerand, A. Sidorova (Petrozavodsk: Karelian Reserch Centre Press), 30–32 (In Russian).

Dauvalter, V. A., Dauvalter, M. V., Saltan, N. V., and Semenov, E. N. (2008). Chemical composition of atmospheric precipitates within the influence zone of the severonikel smelter. *Geochemistry* 10, 1131–1136. doi: 10.1134/S0016702908100108

Dobrovolsky, V. V. (1999). Fine particles of soils as a factor of mass transfer of heavy minerals in the biosphere. *Soil Sci.* 11, 1309–1317. (In Russian).

Ebaid, Y. Y., and Khater, A. M. (2006). Determination of ^{210}Pb in environmental samples. *J. Radioanal. Nuclear Chem.* 270, 609–619. doi: 10.1007/s10967-006-0470-5

Gavshin, V. M., Bobrov, V. A., and Sukhorukov, F. V. (2004). Evidence of the fractionation of chemical elements in the atmosphere of western siberia according to the research of the upper peat bog. *Doklady Russiiskoi Academii Nayk* 396, 804-807. (In Russian).

Geology of the USSA (1997). *Western Siberia. Part I. Geological Description*. Vol. XIV. Nedra, Moscow. (in Russian).

Granina, L. Z. (2008). *Early Diagenesis of Bottom Sediments of Lake Baikal*. Academ. Publishing house "Geo", Novosibirsk (In Russian).

Gurari, F. G., and Gavshin, V. M. (1981). *Planktonic deposits of the Phanerozoic as an indicator of the stability of the content in sea water of rare and radioactive elements. Evolution of the sedimentary process on continents and oceans*. IGiG SBO AN SSSR Press, Novosibirsk, 207–208.

Ilyin, V. V. (1982). Flora and vegetation of manzherok lake (Altai). *Bot J*, 67, 210–220.

Kalugin, I., Darin, A., and Rogosin, D. (2014). "Geochemical signals of paleoclimate recorded in the varved clastic and carbonate lake sediments," in *Paleolimnology of northern Eurasia. Proceedings of the International Conference,* eds D. Subetto, T. Regerand, and A. Sidorova (Petrozavodsk: Karelian Research Centre Press). 47–49. (In Russian). doi: 10.5593/SGEM2013/BD4/S19.018

Kalugin, I., Daryin, A., Smolyaninova, L., Andreev, A., Diekmann, B., and Khlystov, O. (2007). 800-yr-long records of annual air temperature and precipitation over southern Siberia inferred from Teletskoye Lake sediments. *Quat. Res.* 67, 400–410. doi: 10.1016/j.yqres.2007.01.007

Korde, N. V. (1960). *Biostratigraphy and Typology of Russian Sapropels*. Moscow: Publishing House of the USSR Academy of Sciences, 219. (In Russian).

Kutsenogiy, K. P., and Kutsenogiy, P. K. (2000). Aerosols of Siberia. The results of seven years of research. Siberian Ecol. J. VII, 11–20. (In Russian).

Kuzin, I. L. (2007). On the geological role of blue-green algae and the natural conditions of the Precambrian. *News RGO* 139, 48–64. (In Russian).

Leonova, G. A. (2004). Biogeochemical indications of pollution of aquatic ecosystems by heavy metals. *Water Resour.* 31, 215–222. (In Russian). doi: 10.1023/B:WARE.0000021580.73140.51

Leonova, G. A., and Bobrov, V. A. (2012). *Geochemical Role of the Plankton of the Continental Reservoirs of Siberia in the Concentration and Biosedimentation of Microelements*. Academic Publishing House "Hero", Novosibirsk, 308. (In Russian).

Leonova, G. A., Bobrov, V. A., Bogush, A. A., Bychinsky, V. A., and Anoshin, G. N. (2007). Geochemical characteristics of the current state of salt lakes in the altai territory. *Geochemistry* 10, 1114–1128. (In Russian). doi: 10.1134/S0016702907100060

Leonova, G. A., Bobrov, V. A., and Krivonogov, S. K. (2010). "*Biogeochemical Characteristics of Varieties of Lake Sapropels of the Siberian Region. Mineralogy and Geochemistry of Landscapes of Mining Territories*," Modern mineral formation: *Proceedings of the III All-Russian Symposium*. Readings of the memory of Academician A.E. Fersman, November 29 - December 2, 2010. Chita Russia. Publishing house of the Institute of Natural Resources, Ecology and Cryology SB RAS, Chita, 74-78. (In Russian).

Leonova, G. A., Bobrov, V. A., Lazareva, E. V., Bogush, A. A., and Krivonogov, S. K. (2011). Biogenic contribution of microelements to the organic matter of modern lake sapropels (on the example of Lake Kirek). *Lithol. Minerals* 2, 115–131. (In Russian). doi: 10.1134/S0024490211010044

Leonova, G. A., Bobrov, V. A., Lazareva, E. V., and Krivonogov, S. K. (2008). Evaluation of biogenic supply of microelements of lake sapropels (plankton and macrophyte "channels"). Mineralogy and geochemistry of landscapes of mining territories: *Proceedings of the II All-Russian Symposium with International Participation November 10-13, 2008.* Publishing House of the Institute of Natural Resources and Cryology SB RAS, Chita, 70-74. (In Russian).

Leonova, G. A., Bobrov, V. A., and Palesskiy, S. V. (2006). "Use of the elemental composition of plankton and sapropels to estimate the fluxes of matter from the atmosphere (on the example of Lake Kirek, Tomsk Region)," in *Control and rehabilitation of the environment*. eds M. V. Kabanov and A. A. Tikhomirov (Tomsk: Materials of the symposium), 98-100. (In Russian).

Leonova, G. A., and Bychinsky, V. A. (1998). Hydrobionts of the Bratsk water reservoir as objects for monitoring heavy metals. *Water Resour.* 25, 603–610. (In Russian).

Li, Y. -H. (1991). Distribution pattern of the elements in the ocean. *A synthesis. Geochim. Cosmochim. Acta*, 55, 3223–3240. doi: 10.1016/0016-7037(91)90485-N

Lopatko, M. Z. (1978). *The Lake and Sapropel*. Minsk: Science and technology Press.

Malakhov, S. G., and Makhonko, E. P. (1990). Emission of toxic metals and their accumulation in the surface layer of the Earth. *Adv. Chem.* 59, 1777–1798. doi: 10.1070/RC1990v059n11ABEH003575

Moiseenko, T. I., Gashkina, N. A., and Kudryavtseva, L. P. (2006). Zonal features of formation of the chemical composition of the waters of small lakes in the territory of the European part of Russia. *Water Resour.* 33, 163–180. doi: 10.1134/S0097807806020047

Neruchev, S. G. (1982). *Uranium and life in the history of the Earth*. Leningrad: Nedra Press Leningrad branch.

Niu, M., Heaton, T. J., Blackwell, P. G., and Buck, C. E. (2013). The bayesian approach to radiocarbon calibration curve estimation: the IntCal13, Marine13, and SHCal13 methodologies. *Radiocarbon* 55, 1905–1922. doi: 10.2458/azu_js_rc.55.17222

Ogureeva, G. N. (1980). *Botanical Geography of Altai*. Moscow: Nauka Press. (In Russian).

Pawlyta, J., Pazur, A., Piotrowska, N., Poreba, G., Sikorski, J., Szczepanek, M., et al. (2004). Isotopic investigations of uppermost sediments from lake Wigry (NE Poland) and its environment. *Geochronometria*. 23, 71–78.

Perelman, A. I. (1979). *Geochemistry*. Moscow: High school Press (In Russian).

Poplavko, E. M., Ivanov, V. V., Orekhov, V. S., and Tarkhov, Y.A. (1978). Peculiarities of metallicity of combustible shales and some assumptions about their genesis. *Geochemistry* 9, 1411–1418.

Popolzin, A. G. (1967). *Lakes of the South of the Ob-Irtysh Basin (Zonal Complex Characteristic)*. Novosibirsk: West Siberian book publishing house.

Prajith, A., Rao, V. P., and Kessarkar, P. M. (2015). Controls on the distribution and fractionation of yttrium and rare earth elements in core sediments from the Mandovi estuary, western India. *Cont. Shelf Res*. 92, 59–71. doi: 10.1016/j.csr.2014.11.003

Raputa, V. F., Smolyakov, B. S., and Kutsenogiy, K. P. (2000). Analysis of the temporal dynamics of changes in the composition of atmospheric aerosol in the north of Western Siberia. *Siberian Ecol. J.* 1, 97–101.

Reimer, P. J., Bard, E., Bayliss, A., Beck, J. W., Blackwell, P. G., Bronk, R. C., et al. (2013). IntCal13 and Marine13 radiocarbon age calibration curves 0–50,000 years cal BP. *Radiocarbon* 55, 1869–1887. doi: 10.2458/azu_js_rc.55.16947

Rudaya, N., Nazarova, L., Novenko, E., Andreev, A., Kalugin, I., Daryim, A., et al. (2016). Quantitative reconstructions of mid- to late Holocene climate and vegetation in the north-eastern Altai mountains recorded in lake teletskoye. *Glob. Planet. Change* 141, 12–24. doi: 10.1016/j.gloplacha.2016.04.002

Rusanov, G. G., and Vazhov, S. V. (2017). *Unsolved Problems of Lakes Manzherok and Aya*. Biysk, FGBOU VO "AGGGU named after V.V. Shukshina," 168. (in Russian)

Shotyk, W., Cheburkin, A. K., Appleby, P. G., Fankhauser, A., and Kraumers, Y. D. (1996). Two thousand years of atmospheric arsenic, antimony and lead deposition in an ombrotrophic bog profile, Jura Mountains Switzerland. Earth and Planet. *Sci. Lett*. 145, 1–7. doi: 10.1016/S0012-821X(96)00197-5

Smolyakov, B. S. (2000). Problems of acid deposition in the north of Western Siberia. *Siberian Ecol. J. VII* (1), 21–30. doi: 10.1016/S0021-8502(99)80311-5

Steinhilber, F., Beer, J., and Fröhlich, C. (2009). Total solar irradiance during the holocene. *Geophys. Res. Lett*. 36:L19704. doi: 10.1029/2009GL040142

Stuiver, M., and Polach, H. A. (1977). Discussion: reporting of ^{14}C data. *Radiocarbon* 19, 355–363. doi: 10.1017/S0033822200003672

Stuiver, M., and Reimer, P. J. (1993). Extended ^{14}C data base and revised CALIB 3.0 ^{14}C age calibration program. *Radiocarbon* 35, 215–230. doi: 10.1017/S0033822200013904

Suriyanarayanan, S., Brahmanandhan, G. M., Malathi, J., Kumar, S. R., Masilamani, V., Hameed, P. S., et al. (2008). Studies on the distribution of ^{210}Po and ^{210}Pb in the ecosystem of point Calimere coast (Palk Strait), India. *J. Environ. Radioact.* 99, 766–771. doi: 10.1016/j.jenvrad.2007.10.003

Syso, A., and Yu. (2007). *Regularities in the distribution of chemical elements in soil-forming rocks and soils in Western Siberia*. Novosibirsk: SB RAS Press.

Ugur, A., Miquel, J. C., Fowler, S. W., and Appleby, P. (2003). Radiometric dating of sediment cores from a hydrothermal vent zone off Milos Island in the Aegean Sea. *Sci. Total Environ.* 307, 203–214. doi: 10.1016/S0048-9697(02)00542-9

Vetrov, V. A., and Kuznetsova, A. I. (1997). *Microelements in the Natural Environment of Lake Baikal*. Novosibirsk: SB RAS Press, 234.

Vine, J. D., and Tourtelot, E. B. (1970). Geochemistry of black shale deposits. *Econ. Geol*. 65, 253–272. doi: 10.2113/gsecongeo.65.3.253

Wang, W., Ma, Y., Feng, Z., Narantsetseg, T., Liu, K.-B., and Zhai, X. (2010). A prolonged dry mid-Holocene climate revealed by pollen and diatom records from lake ugii nuur in central Mongolia. *Quat. Int*. 229, 74–83. doi: 10.1016/j.quaint.2010.06.005

Xu, F. J., Hu, B. Q., Dou, Y. G., Liu, X. T., Wan, S. M., Xu, Z. K., et al. (2017). Sediment provenance and paleoenvironmental changes in the northwestern shelf mud area of the South China Sea since the mid-Holocene. *Contin. Shelf Res.* 144, 21–30. doi: 10.1016/j.csr.2017.06.013

Xu, X., Trumbore, S. E., Zheng, S., Southon, J. R., McDuffee, K. E., Luttgen, M., et al. (2007). Modifying a sealed tube zinc reduction method for preparation of AMS graphite targets: reducing background and attaining high precision. *Nucl. Instrum. Methods Phys. Res. B* 259, 320–329. doi: 10.1016/j.nimb.2007.01.175

Conflict of Interest: The authors declare that the research was conducted in the absence of any commercial or financial relationships that could be construed as a potential conflict of interest.